Mechanical Systems and Signal Processing 241 (2025) 113539

Contents lists available at ScienceDirect

Mechanical Systems and Signal Processing

journal homepage: www.elsevier.com/locate/ymssp

Advancements in detecting combustion events through vibration analysis in internal combustion engines: a literature review

Zengquan Zheng [a,b], Petros Lappas [b], Amir-Mohammad Shamekhi [a], Xu Wang [b,*], Maciej Mikulski [a]

[a] Efficient Powertrain Solutions (EPS), School of Technology and Innovations, University of Vaasa, Finland
[b] School of Engineering, RMIT University, Australia

ARTICLE INFO

Keyword:
Combustion diagnostics
Source separation
Vibration analysis
Internal combustion engine

ABSTRACT

Accurate combustion characterization is very important for the reliability, efficiency, and emissions of internal combustion engines (ICEs). Standard in-cylinder pressure sensors are costly, obtrusive, and have a short lifespan under harsh environments. This research examines vibration-based analysis as a non-intrusive method for identifying and reconstructing combustion events in compression ignition (CI) and homogeneous charge compression ignition (HCCI) engines. We examine the correlation between engine block vibrations and combustion parameters, including start of combustion (SOC), peak pressure (PP), pressure rise rate (PPRR), maximum heat release rate (HRRmax), and mass fraction burned (MFB), while assessing signal decomposition techniques such as Empirical Mode Decomposition (EMD) and Variational Mode Decomposition (VMD). Advanced signal processing is also combined with machine learning (ML) models to improve real-time estimation and nonlinear mapping.

Our study shows that vibration signals can be used as reliable indicators of combustion, with timing precision of less than 1 CAD and pressure reconstruction error of less than 5%.

Abbreviations: ADMM, alternating direction multiplier method; AGST, adaptive generalized s-transform; ANN, artificial neural networks; ATW, asymmetric Tukey windows; AVMD, adaptive variational mode decomposition; BPF, band-pass filters; BSLM, binaural sound localization method; CAD, crank angle degrees; CHR, cumulated heat release; CI, compression ignition; CS, cepstral smoothing; CWF, cyclic Wiener filter; CWT, continuous wavelet transform; EEMD, ensemble empirical mode decomposition; EMD, empirical mode decomposition technologies; EN, engine noise; ESF, enhanced separation filters; FDM, Fourier Decomposition Method; FEM, finite Element Method; FT, filtering technologies; FuzzDisEn, fuzzy distribution entropy; GRNN, generalized Regression Neural Network; GST, generalized S transform; HCCI, homogeneous charge compression ignition; HHT, hilbert-Huang transform; HPF, high-pass filters; HRR, heat released rate; HRRmax, maximum heat released rate; ICA, independent component analysis; ICEs, internal combustion engines; ICP, in-cylinder pressure; IMEP, indicated mean effective pressure; IMF, intrinsic mode functions; LMA, Levenberg-Marquardt algorithm; LMPV, location of peak velocity; LOPP, location of peak pressure; LPF, low-pass filters; LPP, pressure peak location; MAPE, mean absolute percentage error; MEEMD, modified ensemble empirical mode decomposition; MFB, mass fraction burned; MFB50, half value of the mass fraction burned profile; MFB95, 95% of the fuel mass has burned; ML, machine learning; MoC, middle of combustion; MVDA, multivariate data analysis; NNA, neural Network Analysis; OPME, olive pomace oil methyl ester; PCA, principal Component Analysis; PLS, partial Least Squares; PME, palm oil methyl ester; PP, peak pressure; PPRR, peak pressure rises rate; RBF, radial basis functions; RCCI, reactivity-controlled compression ignition; RMSE, root mean square error; RobustICA, robust independent component analysis; SD, standard deviation; SDOP, second derivative of pressure; SF, separation filter; SOC, start of combustion; ST, s-transform; SPL, sound pressure level; SVM, support vector machines; TDC, top dead center; TF, transform function; TVF-EMD, time varying filter based empirical mode decomposition; VMD, variational mode decomposition technologies; VS, vibration signal; VTDD, variational time-domain decomposition; VTFAD, variational time–frequency adaptive decomposition; WT, wavelet transform.

* Corresponding author.
E-mail addresses: xu.wang@rmit.edu.au (X. Wang), maciej.mikulski@uwasa.fi (M. Mikulski).

https://doi.org/10.1016/j.ymssp.2025.113539
Received 8 March 2025; Received in revised form 11 October 2025; Accepted 18 October 2025

Nonetheless, difficulties persist in adaptive parameter tuning, signal decoupling during transient situations, and the comprehensibility of machine learning models. Hybrid and explainable ML frameworks, multi-sensor data fusion, and the creation of virtual combustion noise sensors for onboard diagnostics are some promising areas of research. In the end, vibration-based combustion analysis provides a cheap and scalable means to get to real-time, non-intrusive monitoring, which will help the shift to cleaner, quieter, and more efficient engines.

1. Introduction

1.1. Monitoring strategies for combustion event detection

Internal combustion engines (ICEs) play a crucial role in transport, powering ships, vehicles and plant. The ability to analyse combustion is essential to optimise engine performance, environmental sustainability and user satisfaction.

It enables researchers to fine-tune parameters like the air–fuel ratio, ignition timing and peak cylinder pressure in order to improve fuel economy, reduce wear and maximise performance. Detecting and addressing issues like knocking and misfires enhances reliability and reduces noise, vibration and harshness (NVH), improving the overall user experience. An enginés efficiency and performance are directly connected to the quality of its combustion. Ongoing ICE innovations, such as direct fuel injection, turbocharging and variable valve timing, create new challenges and opportunities for combustion analysis. Technological advancements influence combustion in unique ways, necessitating comprehensive combustion analysis to maximise benefits and mitigate potential drawbacks.

Real-time monitoring and management of combustion is considered an efficient method to mitigate harmful emissions, reduce fuel consumption and boost thermal efficiency [1]. Normally, combustion inside the cylinder may be monitored by analysing the in-cylinder pressure signal. The primary parameter obtained from in-cylinder pressure measurements is the cycle work and the indicated mean effective pressure (IMEP) [2]. A detailed pressure analysis uses first- or second-law thermodynamic techniques to determine the heat release rate (HRR) as a function of crank angle (CA). Cylinder pressure is a key indicator of the combustion process. Parameters such as the start of combustion (SOC); peak pressure rise rate (PPRR); peak pressure (PP); heat release rate (HRR); and mass fraction burned (MFB) provide insights into efficiency, stability and effectiveness. These metrics help optimise engine performance, reduce emissions and detect faults like misfires or knocking. They collectively offer a comprehensive understanding of combustion dynamics, allowing optimisation of engine design and operation [3].

In-cylinder pressure is typically measured using transducers, but their long-term use is limited by their high cost, susceptibility to errors and degradation under extreme conditions [4]. Maurya and Agarwal [4] showed that, in normal circumstances, a mere movement of one degree in the crank angle of the pressure curve results in a 12 % inaccuracy in determining IMEP. The measurement of maximum heat release rate (HRRmax) normally experiences an error of at least 8 % when one considers the precision of the pressure sensor and take account of the other extra constants, variables and signal transformations involved. Transducers are not reliable for long-term pressure measurements because they have limited durability under high temperatures and pressures.

Consequently, non-intrusive techniques are being increasingly adopted to provide reliable cycle-resolved features and enable scalable field monitoring. These techniques include block vibration, acoustic emission (AE), free- and near-field microphones, instantaneous crankshaft speed and optical or ionization surrogates. Non-intrusive measurement methods using sensors to detect engine instantaneous speed [5], acoustic emissions [6], and surface vibration [7], can be harnessed to observe and analyse combustion.

Vibration measurements are an established means of obtaining signals which contain comprehensive diagnostic information on knock, misfire and combustion phasing [8]. Accelerometers are typically mounted on the cylinder head vertically, i.e., parallel to the cylinder axis. This configuration is based on findings which show vibrations along the cylinder axis carry more direct combustion-related information than signals captured in perpendicular directions [9]. This directional sensitivity significantly influences the fidelity of signal analysis and reconstruction methods. Separating combustion vibration from other cylinders is, in principle, possible when the accelerometer is mounted on the cylinder head or at any other location, but the signal becomes increasingly difficult to decompose. Vibration sensors are widely employed to monitor the state of engines and detect faults in maritime and aviation settings [10]. They are also used extensively in automotive applications to identify knocking combustion in spark ignition (SI) engines [11]. Beyond the scope of engine mechanical condition monitoring and abnormal combustion detection, vibroacoustic technology also contributes to the assessment of combustion characteristics and indirect calculation of in-cylinder pressure.

Acoustic emission (AE) monitoring captures high-frequency structure-borne waves (>100 kHz) generated by rapid energy release events such as knock or pre-ignition [12]. AE methods provide excellent temporal resolution and immunity to low-frequency mechanical noise. However, they require expensive sensors and careful mounting [13].

In contrast, airborne acoustic sensing uses microphones, either free-field or near-field, to record sound radiated into the air from engine surfaces. The free-field microphone is nominally (by standards) placed one metre from the source to capture engine noise in general [14]. The level of challenge in separating combustion instances from free-field noise measurement is further elevated by nonlinearities of the transfer path and cross influence of the environment [15]. If applying near-field microphone techniques, the microphone is usually placed a few millimetres from the source to capture engine noise in a specific direction [16]. This method can be combined with mechanical acoustic insulation to further reduce the interference. To this end, Yao et al [17] for instance, proposed a lead cover method applied to the engine structure to help separation of combustion noise in a marine engine.

Monitoring instantaneous crankshaft speed or torsional vibration offers a cost-effective solution, leveraging existing toothed wheels

and encoders [18]. Each combustion event produces a torque on the crankshaft, causing a slight acceleration in the crankshaft rotation. The expected torque impulse is missing when a misfire occurs, so the crankshaft does not accelerate as much in that cycle. This results in measurable instantaneous angular speed fluctuations at specific crank angles, especially between firing events. It is effective for misfire detection and torque fluctuation analysis but provides limited bandwidth and is influenced by drivetrain dynamics [19].

In addition, optical and ionization-based sensing methods enable detailed study of combustion phenomena. Optical techniques using endoscopes or windowed heads are invaluable for research but impractical in production due to cost and fragility [20]. Ion-current sensing in spark plugs is more feasible for real-time control in spark-ignition engines but requires careful calibration [21].

Overall, these methods present a spectrum of trade-offs. Pressure sensing offers unmatched accuracy but is intrusive and expensive. Vibration sensing provides a balanced combination of cost-effectiveness, durability and diagnostic capability, making it a strong candidate for practical deployment. Table 1 compares different combustion monitoring methods for specific quantities measured and parameters captured, along with their key strengths, limitations, and most suitable applications.

The cited research indicates that there is a strong correlation between cylinder pressure and engine vibration because the rapid change in pressure during combustion causes vibration in the engine block. In other words, vibration data contains important information about the cylinder pressure. Hence, there are possibilities of reconstructing the cylinder pressure from the vibration on the engine block.

Recently, many researchers have taken different approaches to estimate the pressure curve from the accelerometer signal, applied to both spark-ignition and compression-ignition engines. Han et al. proposed and used a recursive method using the Kalman filter algorithm [22]. Bennett and Businaro [23] employed frequency-based coherence analysis to estimate combustion parameters from accelerometer signals.

Intelligent machine learning techniques, such as neural networks and regression network, are increasingly regarded as offering potential to identify combustion events, partially addressing the nonlinearity between cylinder pressure and vibration signals. Bizon et al. [24] have proven artificial neural networks (ANN) to be a reliable method for reconstruction of in-cylinder pressure. Hoang et al. [25] implemented a radial basis function neural network, recurrent and generalised regression networks to reconstruct the cylinder pressure of diesel and gasoline engines with good results. However, there is very little work related to reconstruction of cylinder pressure of homogeneous charge compression ignition (HCCI) engines. Bendu et al. [26] employed regression neural networks to estimate combustion parameter demonstrating their effectiveness as a tool for studying combustion in HCCI engines.

1.2. Overview of vibration decomposition techniques for identifying combustion-related excitations

Vibration analysis is a promising alternative to traditional in-cylinder pressure measurements because of its strong correlation with combustion dynamics. However, despite significant advancements in identifying key combustion parameters, several challenges remain when using vibration analysis to detect combustion events. One major challenge is the inherent complexity and variability of ICE operations, which can affect the consistency and accuracy of vibration-based methods when applied across a variety of engines. Additionally, external factors such as engine load, speed and environmental conditions can introduce noise which complicates the analysis and increases the difficulty of real-time monitoring. Techniques such as blind source separation (BSS) [22] and filtering technologies (FT) [23] like Fourier transforms and the Cyclic Wiener filter (CWF) [24] are commonly used to analyse engine vibration sources. Liu et al. [16] separated vibration sources by blind source separation techniques and proposed a combination of the blind least mean square algorithm with a deflation method to separate several sources.

Nevertheless, the disentanglement of overlapping frequency components remains challenging due to the close interconnection of sources such as concurrent combustion and mechanical impacts. Sophisticated signal decomposition methodologies have emerged as highly effective tools to address this. Empirical mode decomposition (EMD) [27], variational mode decomposition (VMD) [28], wavelet transforms (WT) [29], and ensemble-based methods [30] enable to break down complex acoustic signals into intrinsic components, thereby increasing the identification accuracy of the combustion induced vibration.

Recent studies show that combining machine learning (ML) and artificial intelligence (AI) with decomposition methods significantly improves their practical applications [29,30,31]. These hybrid methods combine data-driven learning with adaptive decomposition to automate feature extraction, improve classification accuracy, and support real-time monitoring. This integration is becoming central to modern combustion noise research.

Notably, these noise separation methods have been implemented, to some extent, for isolating combustion noise in internal combustion engines. However, other methods like independent component analysis (ICA) [32] have not yet been directly applied to this area. Other potential applications, such as fault diagnosis, fall outside the scope of this work, but the separation techniques presented here may provide a valuable foundation for future research in these related areas. For instance, Zhao et al. [31] established variational time–frequency adaptive decomposition (VTFAD) for multi-impact vibration signals to decompose and extract single-impact components for crankshaft bearing diagnosis. Yang et al. [32] introduced a discriminative non-negative matrix factorisation (DNMF) algorithm designed specifically for image-based fault diagnosis. These methods balance accuracy and computational efficiency, making real-time combustion monitoring feasible in advanced engine systems.

1.3. Motivation objective, methods and scope of the review

The previous subsections assert that combustion can be identified and controlled by a vibration signal. The technology is relatively well-established in spark-ignited engine control in light-duty applications, and provides robustness benefits over in-cylinder-pressure sensing. But there has been only limited application in heavy-duty engines, hindered by both phenomenological complexity of the

Table 1
Comparative analysis of combustion monitoring methods.

Method	Intrusiveness	Cost	Bandwidth	Outputs	Advantages	Disadvantages	Typical Applications
In-cylinder pressure	High	High	Very High	Pressure trace, HRR, IMEP	Most accurate; gold standard for research	Intrusive; expensive; thermal drift; short lifespan	Research, calibration
Surface vibration	Low	Low–Medium	High	Knock/misfire, pressure proxies	Non-intrusive; robust; scalable for field monitoring	Indirect measurement; transfer path effects; requires advanced processing	Condition monitoring, prognostics
Acoustic emission (AE)	Low	Medium–High	Very High	High-frequency events	Excellent temporal resolution; detects early anomalies	Specialized sensors; sensitive to mounting; costly	Abnormal combustion detection
Airborne acoustic	None	Low	Medium	SPL*, noise signatures	Non-contact; very easy deployment	Highly noise-sensitive; poor precision for cycle analysis	NVH analysis, coarse combustion state
Crankshaft speed/ torsion	Low	Low	Low–Medium	IMEP variation, misfire flags	Low cost; reuses existing hardware	Limited bandwidth; influenced by drivetrain dynamics	Fleet-level monitoring
Optical / ionization	Medium–High	Medium–High	High	Flame imaging, ion current	Rich combustion detail; ion probes allow real-time control	Complex setup; calibration-sensitive; fragile optics	Research, spark-ignition control

* Sound pressure level.

combustion process, its control and the entanglement of vibration spectra.

The complexity of conventional diesel combustion arises from multi-pulse injections, resulting in a heat release pattern which becomes difficult to identify with indirect methods [33]. Combustion becomes even more complex in advanced low-temperature, compression-ignition engines, which are key to next-generation, ultra-low-emission designs [34]. Here the mixture ignition lacks direct control authority from either spark or ignited liquid spray, making combustion sensing necessary for feedback and model predictive control [35].

The complexity of vibration spectra is further increased by the overlapping effect of valve-train, injection armature and piston-slap excitations, stemming from much higher mechanical forces exerted by heavy-duty engines [36]. But the recent emergence of modern signal separation techniques opens up new opportunities to use vibration analysis for combustion control. To date, no comprehensive review has systematically organised these advanced applications, making it hard to apply solutions across different engine platforms.

For instance, Chu et al. [37] provided a comprehensive overview of vibration analysis applications, but omitted the particulars of combustion event detection in internal combustion engines. Karabacak [38] examined machine learning techniques for detecting faults in internal combustion engine vibration signals, but the research was restricted to certain fault categories and did not encompass a broader spectrum of combustion control applications. These gaps highlight the absence of a comprehensive, contemporary review which consolidates decomposition techniques, signal correlation methods, and intelligent reconstruction algorithms specifically designed for combustion event detection, especially concerning compression ignition (CI) and homogeneous charge compression ignition (HCCI) engines.

The present study aims to tackle these knowledge gaps. It has the following overarching research objectives, substantiating both fundamental relevance and applied significance of the sought systematisation:

- Quantify the correlation between combustion parameters and engine block vibration signals, with particular attention to SOC, PP, PPRR, HRR and MFB

  Objective metric: measurement and comparison of estimate errors for every parameter (e.g., SOC estimation error < 0.9 CAD, HRRmax location error ≤ 1 CAD, LOPP estimation error ≤ 0.9 CAD)

- Methodically assess, for CI and HCCI engines, the efficiency of signal decomposition methods (e.g., FT, EMD, VMD) for isolating combustion-induced vibrations from mechanical noise sources

  Objective metric: benchmarking signal separation accuracy using combustion parameter estimation errors yields an objective metric

- Determine and rank vibration-based combustion quantifiers best fit for real-time combustion monitoring in engines using compression ignition

  Objective metric: Average estimation error, signal-to– noise ratio, and implementation cost guide priorities

- Evaluate how advanced combustion modes (e.g., LTC, HCCI, RCCI) affect the accuracy and interpretability of vibration-based data processing systems, particularly under transient engine conditions

  Objective metric: evaluation of error deviation ranges for PPRR, HRRmax, MFB50 throughout several combustion modes

- Review and integrate machine learning (ML) and neural network (NN) models (e.g., RBF, GRNN, BPANN) with advanced signal separation techniques to facilitate precise identification of combustion-induced excitations

  Objective metric: quantitative comparison of RMSE values for combustion parameters (e.g., SOC estimation error < 0.9 CAD, HRRmax location error ≤ 1 CAD, PP estimation error ≤ 0.9 CAD)

We used a methodical literature review approach to address these goals. Comprehensive keyword searches in scholarly databases, including Scopus and Google Scholar, turned in an initial pool of 260 papers about vibration analysis in internal combustion engine applications. Keywords employed were “vibration combustion identification,” “combustion process detection” and “combustion noise separation.” Lack of attention to combustion-related vibrations led to 137 research being removed following an initial title and abstract screening. Among the remaining 123 papers, eight concentrated soley on spark-ignition engines and knock detection, an area previously well-covered, so were omitted to keep the focus on advanced combustion analysis for CI and HCCI engines. Full-text reviews led to the elimination of 30 more papers due to methodological flaws or inadequate outcome reporting. Using citation monitoring, a further 18 excellent research papers were then added, making a total of 103 core papers for this review. This method of structured filtering guaranteed inclusion of only thorough, high-impact research pertinent to combustion process detection and combustion-induced vibration analysis.

This review article is methodically organised to assist the main goal of identification, quantification and reconstruction of combustion-related events in internal combustion engines by means of non-intrusive vibration analysis. Section 2 investigates the relationship between combustion quantifiers (e.g., SOC, PP, PPRR, HRRmax, and MFB) and engine vibration. These findings enable accurate and real-time combustion characterisation through vibration signals. Furthermore, the ability to use decomposition methods

to separate combustion-induced excitation is needed to increase prediction accuracy. Therefore, section 3 reviews various filtering and advanced signal decomposition methods employed for ICEs. And the review includes a machine learning-based method for combustion noise prediction, which helps vibrational data to be more interpretable, especially in complicated scenarios like overlapping mechanical vibrations or multi-pulse injections. Section 4 provides a critical review of the studieś findings and evaluates them in terms of estimation accuracy, robustness across engine types and suitability for real-time applications. Practical challenges and future directions are also investigated. Finally, section 5 presents the conclusions, summarising the reviewś key findings.

2. Correlation between cylinder pressure and vibration

As previously discussed, vibration signals can be used to detect the combustion process by either recreating the in-cylinder pressure curve or using combustion quantifiers. Signal decomposition methods help isolate combustion-related components from general engine vibrations, improving identification accuracy. Fig. 1 shows the general framework for identifying combustion events.

2.1. Combustion quantifiers

The rapid pressure fluctuations inside the combustion chamber excite vibrations that can be detected on the engine block, reflecting a strong relationship between in-cylinder pressure variations and engine vibrations. Effective identification of combustion processes relies on distinct signal characteristics, including the start of combustion, peak pressure, peak pressure rise rate, maximum heat release rate, and mass fraction burned. Separation techniques help isolate combustion-induced vibrations from other mechanical noise sources, improving accuracy in combustion event detection.

2.1.1. Start of combustion

The ignition of the air–fuel mixture is a critical step that initiates power generation in an internal combustion engine. Heat is released due to rapid combustion when the air–fuel mixture ignites. Consequently, the start of combustion occurs somewhat before the release of heat. Fig. 2 displays the filtered accelerometer trace and the cumulative heat release (CHR) curve. The data for each was normalised by dividing the respective maximum values. The start of the heat emission is indicated by the green dashed line in Fig. 2. The SOC is a critical phase in an ICE, marking the ignition of the air–fuel mixture and the start of power generation. The SOC is typically identified through the zero-crossing point of the filtered accelerometer trace, which aligns closely with the theoretical SOC location.

For ease of estimation, Chiatti et al. [39] identified this zero-crossing point of the filtered acceleration trace as SOC. Several studies have validated this method, achieving estimation errors within 1.38 crank angle degrees (CAD).

Knocking, also known as detonation, pinging or pinking, occurs in spark-ignition (SI) engines when part of the air–fuel mixture ignites abnormally. Instead of burning through the flame front initiated by the spark plug, it explodes outside the normal combustion envelope. The engine experiences brief structural vibrations due to knocking. In such cases, the transient vibration velocity amplitude increases significantly, corresponding to the onset of rapid pressure rise [40]. In Fig. 3, both the vibration velocity signal and the pressure rise rate contain the feature points pertaining to the combustion process. The location of the SOC was traditionally understood to be the knee point of the pressure rise rate curve (point A) during the compression stroke [41]. Accordingly, SOC was identified using the A' in the revised vibration velocity. The engine vibrates because of a sudden shift in cylinder pressure brought on by fuel burning. Thus, the start of combustion aligns with the engine vibration change (A') and the inflection point (A) in the pressure rise rate curve, marking the onset of cylinder pressure change.

For ease of estimation, Zhao et al. [42] identified the zero-crossing point of the engine vibration velocity as SOC. A systematic bias exists, with SOC determined from vibration velocity (SOCV) lagging that from the pressure rise rate curve (SOCP) by an average of 1.3

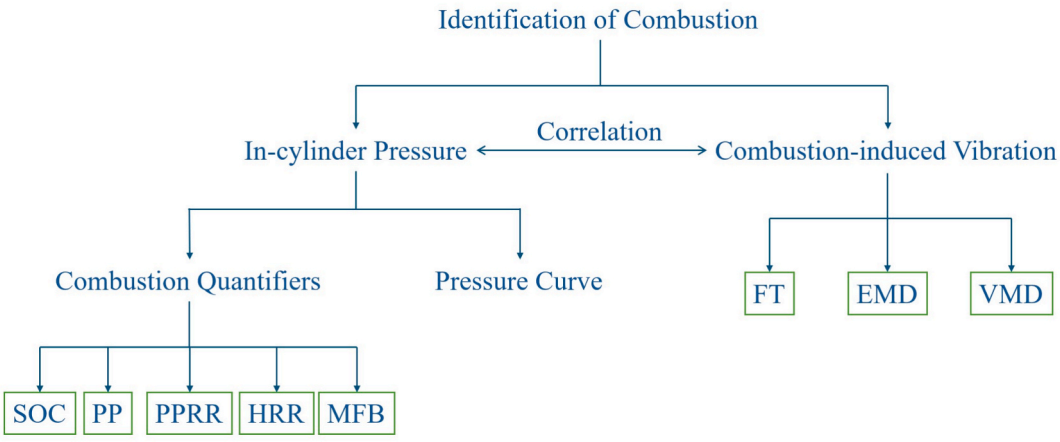

Fig. 1. Framework of identification of combustion event.

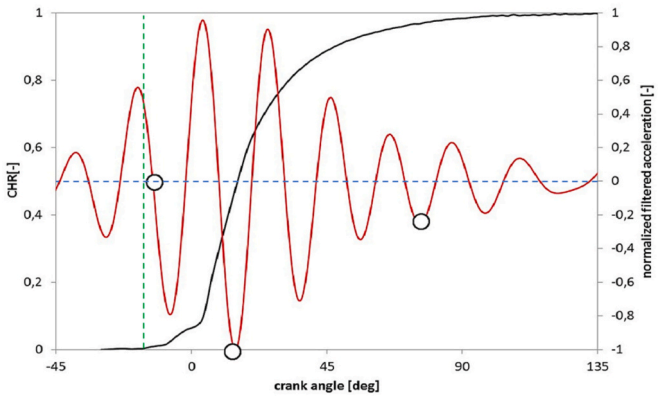

Fig. 2. Cumulated heat release curve (black) and filtered accelerometer trace (red) (3200 rpm, 100 % load) [39]. (Reproduced from Energy with permission from Elsevier).

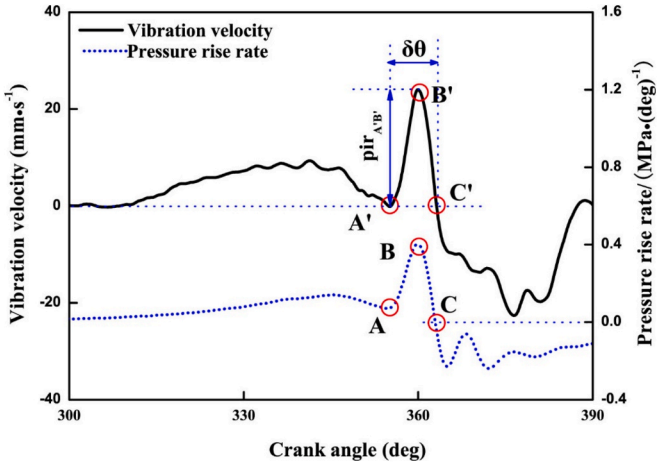

Fig. 3. Recognition schematic of the combustion parameters [42]. (Reproduced from Journal of Sound and Vibration with permission from Elsevier).

CAD. The error of the anticipated SOC when the SOCV is corrected with this system bias is within 1.1 CAD when compared to the SOCP under various operating conditions. The similar technique was employed by Ji et al. [40] and Yang et al. [43] to determine SOC from engine surface vibration signals, with maximum errors of 0.9 CAD and 2 CAD, respectively. All the previously mentioned research works are in a CI engine. Cheng et al. [44] estimated SOC from vibration using homogeneous charge compression ignition (HCCI) engine, with errors ranging from 2.4 CAD to 3.3 CAD. Table 2 lists different SOC identifications that were discussed in the literature.

As shown in Table 2, SOC for both HCCI and CI engines is typically determined using either the zero-crossing point of the velocity or acceleration signals, or the inflection point on the vibration velocity signal. Additionally, the SOC estimation accuracy of the CI engine is greater than that of the HCCI engine due to the volumetric combustion of an HCCI engine producing a high PRR, which results in a

Table 2
Summary of SOC estimation.

Ref.	Year	Engine Type	Operating conditions	Vibration sensor	Analytical approach	Error, remarks
[44]	2012	HCCI, 2-cylinder; 1630 cm^3	1200–1600 rpm	Velocity sensor GST CS-YD-005, 4–4000 Hz	Time domain, the first bending/ inflection point on velocity curve	varied from 2.4 CAD to 3.3 CAD
[39]	2017	CI, 3-cylinder, 1028 cm^3	1600–3600 rpm; 0.24–0.62 MPa (BMEP)	Accelerometer Endevco 7240C, max. 5000 Hz	Time domain, zero-crossing point on acceleration curve (Fig. 2)	1.38 CAD (mean absolute error)
[42]	2017	CI, 1-cylinder, 815 cm^3	800–1400 rpm; 0.15–0.77 MPa (BMEP)	Velocity sensor GST CS-YD-005, 4–4000 Hz	Empirical mode decomposition, zero-crossing point on velocity curve (Fig. 3)	1.1 CAD (max error)
[40]	2021	CI, 12-cylinder, 71450 cm^3	1200–1500 rpm, 0.14–1.1 MPa (IMEP)	Accelerometer GST CA-YD-102, 0.5–10000 Hz	Time domain, zero-crossing point on acceleration curve	2 CAD (max error)
[43]	2022	CI, 1-cylinder, 815 cm^3	800–1400 rpm; 0.15–0.77 Mpa;(BMEP)	Accelerometer GST CA-YD-102, 0.5–10000 Hz	Fourier decomposition method, zero-crossing point before peak acceleration	0.9 CAD (max error)

more pronounced vibration amplitude. Advanced separation techniques help isolate combustion-induced vibrations more precisely, reducing SOC estimation errors. Yang et al. [43] produced the minimum SOC error of 0.9 CAD by using a GST CA-YD-102 accelerometer to measure vibration in 1-cylinder, 0.815-litre CI engine operating at 800–1400 rpm. The Fourier decomposition method was applied, using the zero-crossing point before peak acceleration.

2.1.2. Peak pressure (PP)

Peak cylinder pressure is directly linked to engine power output. Higher peak pressures indicate more efficient combustion. PP can be estimated using vibration signals by analysing zero-crossing points in velocity curves or identifying minimum points following peak acceleration. The estimation error typically remains within 0.8 CAD.

Zhao et al. [42] compared vibration velocity and pressure rise rate. They considered the first crossing zero point (point C in Fig. 3) after peak value of the peak pressure rise rate as the location of peak pressure which correspondingly was estimated using the C' point in renovated vibration velocity. Importantly, there existed angle deviations between location of peak pressure (LPP) point C and location of zero-crossing point C' in the vibration velocity curve (LPV), as shown in Fig. 4. Furthermore, the deviation angle is not constant. The angle interval δθ, which represents the combustion duration and is seen in Fig. 3, is inserted to correct the deviation. The statistical findings indicate that the error margin between the anticipated LPV and the actual LPP remains within 0.8 CAD under the specified test conditions.

Depicted in Fig. 5, Yang considered the minimum point (C2) of the filtered acceleration after the peak value of the SDOP curve (Fig. 5(b)) as the estimation of PP (Fig. 5(a)). $p(\theta_{C1})$ represents the peak pressure, so $p'(\theta_{C1})$ is equal to zero, where θ_{C1} is the crank angle at point C1. Nonetheless, $p''(\theta_{C1})$ is neither an extremum (highest or minimum) nor zero, rendering the identification of C1 and the determination of location of peak pressure (LOPP) through direct use of second derivative of pressure (SDOP) extremely challenging. The minimum point (C2) of the filtered acceleration following the peak cylinder pressure value is situated near the crank angle of C1 and is easily identifiable. C2 could be utilised to identify LOPP. The findings indicated that the greatest disparity across various engine operating conditions was 0.9 CAD.

Differently, in Ji et al. [45], the summation of frequency amplitude estimated by the S-transform (ST) method in a selected frequency range (200–600 Hz) was employed to identify PP. The maximum relative error of the estimated PP compared to the measured value was −4.93 %.

Table 3 compares each of the PP identifications that were discussed. Theoretically, the criteria for identifying the position of PP in all examined articles are consistent, defined as the initial zero-crossing point subsequent to peak velocity, or alternatively, the minimal point following peak acceleration. Their selection is straightforward, so the accuracy of LOPP estimation appears favourable. The LOPP combustion quantifier is predominantly employed in CI engines: the rapid combustion in HCCI engines hinders the study of their PRR. The estimation error of the PRR value necessitates improvement.

2.1.3. Peak pressure rises rate (PPRR)

Peak pressure rises rate reflects the rate at which cylinder pressure increases during combustion. It influences engine performance and knock propensity. PPRR can be identified using peak velocity points or the first zero-crossing point after peak acceleration. Methods such as summation of frequency amplitude improve estimation accuracy.

The pressure rise rate (PRR) in an internal combustion engine denotes the velocity at which in-cylinder pressure escalates during combustion, commonly quantified in measures such as bar per degree of crank angle or bar per millisecond [2]. A rapid combustion process results in a sudden increase in pressure, whereas a slower combustion yields a more gradual rise in pressure. This metric is crucial in reflecting the dynamics of the combustion process, affecting performance, efficiency, and overall engine functioning.

The location of peak velocity (LMPV) (Point B' in Fig. 3) [42] can be used to identify the location of PPRR (LMPP) (Point B in Fig. 3).

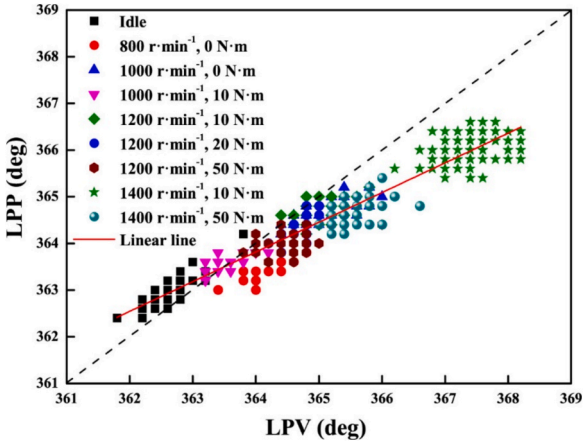

Fig. 4. LPPs (point C' in Fig. 3) LPVs (point C in Fig. 3) at different working conditions [42]. (Reproduced from Journal of Sound and Vibration with permission from Elsevier).

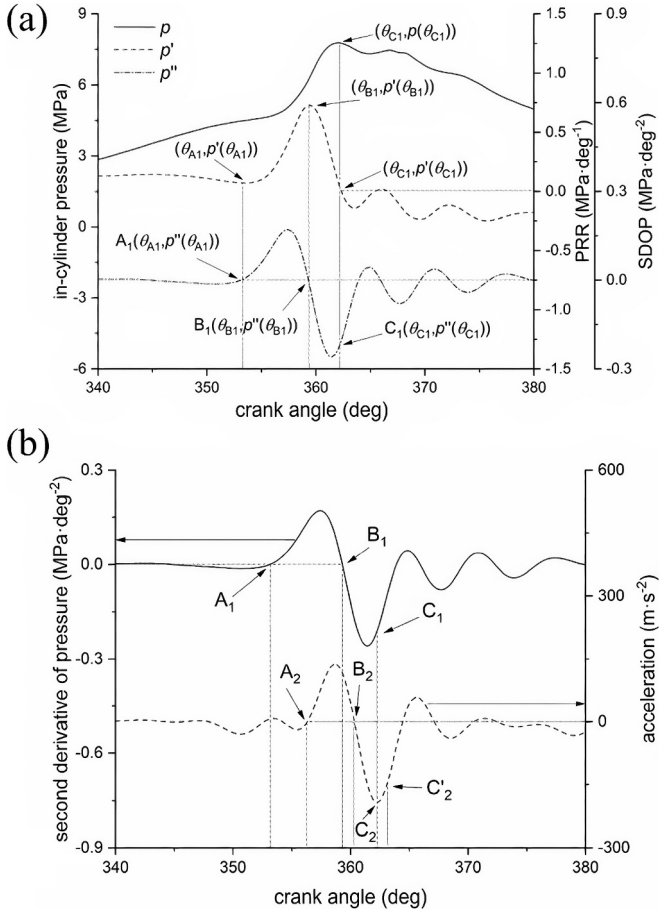

Fig. 5. (a) Some feature points on the curve of SDOP; and (b) comparison of feature points on the curve of SDOP and filtered acceleration [43]. (Reproduced from International Journal of Engine Research with permission from Sage Publications).

Table 3
Summary of PP estimation.

Ref.	Year	Engine Type	Operating conditions	Vibration sensor	Analytical approach	Error, remarks
[42]	2017	CI, 1-cylinder, 815 cm3	800–1400 rpm; 0.15–0.77 MPa (BMEP)	Velocity sensor GST CS-YD-005, 4–4000 Hz	Empirical mode decomposition, zero-crossing point following peak velocity	0.8 CAD (location, max error)
[43]	2022	CI, 1-cylinder, 815 cm3	800–1400 rpm; 0.15–0.77 Mpa; (BMEP)	Accelerometer GST CA-YD-102, 0.5–10000 Hz	Fourier decomposition method, minimum point (C2) after the peak acceleration	0.9 CAD (location, max error)
[45]	2018	CI, 12-cylinder, 71450 cm3	1200–1500 rpm, 0.14–1.1 MPa (IMEP)	Accelerometer GST CA-YD-102, 0.5–10000 Hz	ST, summation of frequency amplitude	−4.93 % (value, maximum relative error)

Fig. 6 indicates angle deviations between LMPVs (Point B2 in Fig. 5(b)) and LMPPs (Point B1 in Fig. 5(a) and 5(b)). Consequently, the combustion process intensity, $pir_{A'B'}$, is introduced to rectify the deviation. The $pir_{A'B'}$ is characterised as the increment from the knee point to the peak value point in the vibration velocity signal, as seen in Fig. 3, specifically representing the proportion of high frequency. The statistical findings indicate that the error margin between the anticipated LPV and the actual LPP remains within 0.6 CAD under the specified test conditions.

Ji et al. [40] initially created a dynamic finite element method (FEM) model to validate the correlation between combustion pressure and vibration time periods. Consequently, they suggested a rapid processing technique to determine the position of the peak pressure rise rate (PPRR) by identifying the first zero-crossing point following peak acceleration, as illustrated by φ_{pir} and $\varphi_{pir'}$ in Fig. 7. The average value of the deviation was 0.82 CAD. Using the same definition of the location of PPRR, Yang et al. [43] employed Fourier decomposition method (FDM) to extract combustion-induced vibration signals from engine surface vibration measurements. The

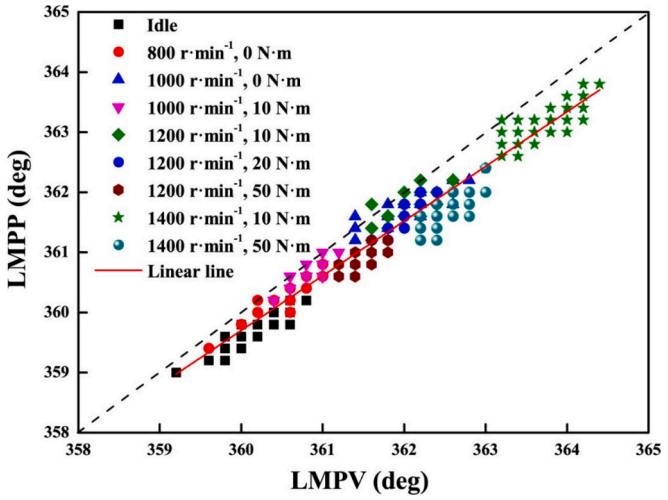

Fig. 6. LMPPs (Point B in Fig. 3) and LMPVs (Point B' in Fig. 3) at different working conditions [42]. (Reproduced from Journal of Sound and Vibration with permission from Elsevier).

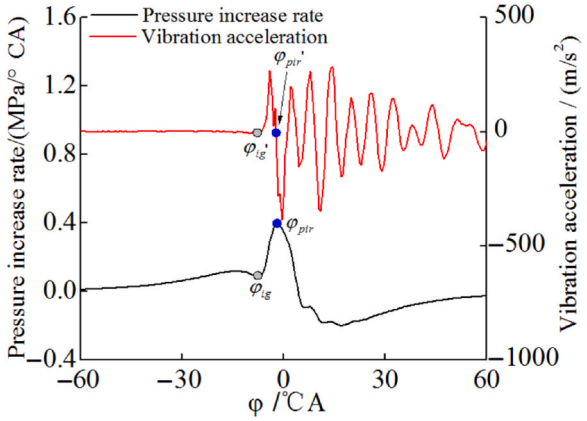

Fig. 7. Comparison of PRR and vibration acceleration [40]. (Open Access).

findings indicated that the greatest disparity across various engine operating conditions was 0.7 CAD. Differently, Ji et al. [45] employed the summation of frequency amplitude estimated by ST method in a selected frequency range (200–600 Hz) to identify PPRR. The maximum relative error of the estimated PPRR compared to the measured value was 6.69 %.

Table 4 compares each of the PPRR identifications that were discussed. The application of the separation approach to handle vibration signals enhances the accuracy of PPRR identification. The PPRR combustion quantifier is used primarily in CI engines: the quick combustion of HCCI engines complicates the analysis of their PRR. Both the location of peak velocity and first zero-crossing point

Table 4
Summary of PPRR estimation.

Ref.	Year	Engine Type	Operating conditions	Vibration sensor	Analytical approach	Error, remarks
[42]	2017	CI, 1-cylinder, 815 cm3	800–1400 rpm; 0.15–0.77 MPa (BMEP)	Velocity sensor GST CS-YD-005, 4–4000 Hz	Empirical mode decomposition, peak velocity	0.6 CAD (location, max error)
[40]	2021	CI, 12-cylinder, 71450 cm3	1200–1500 rpm, 0.14–1.1 MPa (IMEP)	Accelerometer GST CA-YD-102, 0.5–10000 Hz	Time domain, zero-crossing point after peak acceleration	2 CAD (location, max error)
[43]	2022	CI, 1-cylinder, 815 cm3	800–1400 rpm; 0.15–0.77 Mpa; (BMEP)	Accelerometer GST CA-YD-102, 0.5–10000 Hz	Fourier decomposition method, zero-crossing point after peak acceleration	0.7 CAD (location, max error)
[45]	2018	CI, 12-cylinder, 71450 cm3	1200–1500 rpm, 0.14–1.1 MPa (IMEP)	Accelerometer GST CA-YD-102, 0.5–10000 Hz	ST, summation of frequency amplitude	6.69 % (value, maximum relative error)

following peak acceleration can be defined as the location of PPRR. The estimation error of the PPRR value requires enhancement.

2.1.4. Maximum heat released rate (HRR_{max})

HRRmax is associated with combustion intensity and energy release. Studies have shown a strong correlation between HRRmax and engine block vibrations, particularly within specific frequency ranges. Estimation techniques, including continuous wavelet transform (CWT) and bandpass filtering, have been employed to extract HRRmax values with high accuracy.

The heat released rate (HRR) curve illustrates the combustion rate of the air–fuel mixture and the energy released throughout the combustion cycle. It offers insight into combustion stages like ignition delay, premixed combustion, and diffusion-controlled combustion [2].

Lee et al. [46] demonstrated that the maximum heat release rate (HRRmax) has a significant association with the intensity of engine block vibrations, especially within the frequency range of 0.3–1.5 kHz. The vibrations occurring within 35 CAD post-injection ignition greatly impacted the HRRmax. The determination coefficient was 0.892. Jacek et al. [29] employed the peak acceleration with bandpass filter to evaluate the HRRmax. The research precisely identified the HRRmax position within 1 CAD when the vibration amplitude surpassed a threshold of 100 m/s^2, including 98.5 % of the examined combustion cycles. The greatest error in peak HRR prediction accuracy was below 21 %, making it appropriate for monitoring response rates, particularly in cases of incomplete combustion and high ringing cycles. The model for predicting combustion time (HRRmax location) exhibited diminished accuracy at elevated speeds, recording a maximum median absolute error of 0.62 CAD at the operating point characterised by the greatest combustion variability.

Table 5 compares the two HRRmax identifications that were discussed. Currently, there is limited research that demonstrates the correlation between HRRmax and vibration. Nonetheless, based on the findings of the two studies, the precision of employing vibration to forecast HRRmax remains significantly high, even in the absence of improved technology to isolate combustion-induced vibration signals from the measured vibration signals.

2.1.5. Mass fraction burned (MFB)

MFB quantifies combustion progress, with MFB50 indicating optimal combustion phasing. MFB can be estimated through Gaussian function coefficients or identified through minima in filtered acceleration curves. The estimation error for MFB50 and MFB95 is typically around 1.3 CAD.

Mass fraction burned (MFB), a normalised quantity on a scale from 0 to 1, describes the release of chemical energy as a function of crank angle in each engine cycle [47]. The half value of the MFB profile (MFB50) is the most intriguing feature. It indicates that 50 % energy conversion happens at 8 CAD after TDC, which is theoretically the optimal engine combustion efficiency. Fig. 8 effectively illustrates the meaning of MFB50 [29]. The precise crank angle location of the 50 % energy conversion needs to be determined and adjusted by changing the ignition point/spark ignition advance angle.

Chauvin et al. [48] employed Gaussian probability function to estimate the shape of the most relevant part of the signal and MFB50 could be defined as the centre of the function. Even at low-load operating points in HCCI mode, where the noise level is very low (82 dB), the extraction of the middle point of combustion (MoC) succeeds. The proposed method can accurately estimate MFB50, with a standard deviation under 5 CAD compared to the values computed from the cylinder pressure signal, even in HCCI mode. However, a small variation on MFB50 is amplified at the middle point of combustion on the knock sensor. Chiatti et al. [39] considered the absolute minimum in the vibration as MFB50 which simplified the calculation. The crank angle at which 95 % of the fuel mass has burned is designated as MFB95. This metric is employed to evaluate the degree of combustion completion. The reduction of unburned hydrocarbons and other pollutants, along with the timely occurrence of MFB95, contribute to cleaner engine running. Therefore, Chiatti et al. [39] considered the following third minimum in the accelerometer oscillation as MFB95, which is the third point in Fig. 2 [39]. The correlation coefficient (R^2) between the combustion parameters determined from the accelerometer signal and the in-cylinder pressure measurements was very high, close to unity. The results show that this approach can be effectively used in control algorithms to optimize the combustion phasing across multiple cylinders. The maximum deviations of the MFB50 and MFB95 are 1.32 CAD and 1.29 CAD respectively.

Table 6 compares the two MFB identifications that were discussed. It is clear that MFB can be estimated either by Gaussian function coefficient or the corresponding minimum values in the filtered vibration acceleration curve. Importantly, despite the great accuracy for CI engines, there is less study of MFB to analyse combustion progress because of the complex calculation. Furthermore, the rapid combustion with high heat release rates of HCCI results in a large MFB estimation inaccuracy in these engines.

Table 5
Summary of HRR_{max} estimation.

Ref.	Year	Engine Type	Operating conditions	Vibration sensor	Analytical approach	Error, remarks
[46]	2015	CI, 4-cylinder, 1600 cm^3	1250–2000 rpm; 0.4–0.8 MPa (BMEP)	Accelerometer Kistler 8728A, 2–10000 Hz	CWT, cumulative value between 0.3 and 1.5 KHz	peak HRR: $R^2 = 0.892$
[29]	2023	HCCI, 1-cylinder, 499 cm^3	900–2300 rpm; 0.18–0.53 Mpa;(gross IMEP)	Accelerometer PCB ICP M338A34, 0.7–3000 Hz	bandpass filter, time domain, the first maximum point on acceleration wave	Location of peak HRR: 0.62 CAD (mean absolute error); peak HRR: 21 % (mean absolute error)

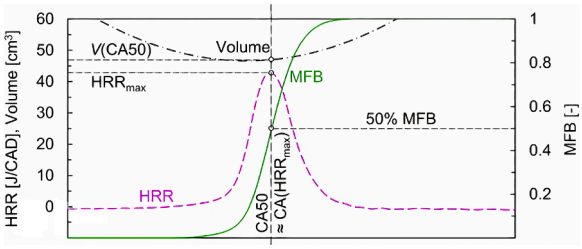

Fig. 8. Exemplary in-cylinder pressure with calculated HRR and MFB functions, cylinder volume [29]. (Reproduced from Energy Conversion and Management with permission from Elsevier).

Table 6
Summary of MFB estimation.

Ref.	Year	Engine Type	Operating conditions	Vibration sensor	Analytical approach	Error, remarks
[48]	2008	HCCI, 4-cylinder, light-duty	1000–1500; 0.1–0.6 MPa (IMEP)	Acceleration-type knock sensor	Gaussian function coefficient fit to instantaneous vibration energy, 1.5–3 kHz	standard deviation under 5 CAD
[39]	2017	CI, 3-cylinder, 1028 cm^3	1600–3600 rpm; 0.24–0.62 MPa (BMEP)	Accelerometer Endevco 7240C, max. 5000 Hz	MFB50: absolute minimum; MFB95: the following third minimum	MFB50: 1.32 CAD (mean absolute error), MFB95: 1.29 CAD (mean absolute error)

2.2. Characterization of in-cylinder pressure dynamics

While global combustion indicators discussed in Section 2.1 provide essential information on combustion phasing and efficiency, they represent only the macroscopic features of in-cylinder thermodynamic evolution. A more comprehensive understanding of combustion behaviour requires examining the dynamic characteristics of the in-cylinder pressure signal, which encompasses both the smooth pressure rise associated with bulk heat release and the superimposed high-frequency oscillations caused by vibro-acoustic resonance [49] and rapid energy discharge [50]. These dynamic pressure components are directly responsible for the vibration signatures captured on the engine block and therefore serve as the physical foundation linking combustion processes with vibration-based diagnostics [51,52].

This section looks at analytical methods that describe how pressure changes inside a cylinder from two different points of view. Section 2.2.1 discusses rebuilding the cylinder-pressure trace. It focuses on how vibration or other data can be used to get a very accurate picture of how the pressure changes over time. Section 2.2.2 goes into more detail about the study of pressure oscillations caused by combustion, focusing on their physical causes, spectral properties, and advanced time–frequency methods such as the adaptive generalized s-transform (AGST) [53] that make it possible to accurately identify these oscillatory phenomena. These methods work together to give a multiscale picture of how pressure behaves in a cylinder, which makes them an analytical link between thermodynamic combustion events and associated vibration responses.

2.2.1. Reconstruction of cylinder pressure trace

Recent studies have explored various approaches to reconstruct cylinder pressure curves using vibration signals. Traditional methods rely on frequency domain analysis, while modern techniques leverage machine learning models such as radial basis function (RBF) networks and generalised regression neural networks (GRNN). These models demonstrate high accuracy in predicting peak pressure values and combustion phasing across various operating conditions.

Estimation of the averaged combustion pressure waveform over multiple cycles was attempted by DeJong et al. [54], Lyon and Jeung [55], Azzoni et al [56], and Bowen [57]. Furthermore, Lyon's approach proved to be ineffective for spark-ignition engines, despite being suitable for diesel engines. This was because spark-ignition engines have lower combustion pressures and, consequently, lower signal levels. An extension of these findings by Piero makes it possible to rebuild the cylinder pressure waveform cycle-by-cycle during free accelerations, without having to know the engine load and coupling parameters [58]. The crucial factor is that, within an angular range centered on the cylinder's top dead center position, there is a considerable linear link between cylinder indicated pressure and engine block vibration. It demonstrated that the order frequency domain's first few harmonics of the cylinder indicated pressure can accurately depict the pressure waveform and offers a straightforward method for calculating the frequency response function (FRF) that connects the vibration and pressure signals. Cycles in which the average engine speed differs significantly from the nominal value used in the FRF estimation procedure result in a lower quality reconstruction of the pressure waveform. More testing is necessary to confirm that the FRFs calculated for one engine can be applied to other engines in the same production line.

Gao [59] suggests a novel time-domain smoothing method to lessen the impact of transfer function changes. This method assesses the transfer function along a line parallel to the frequency axis in the s-plane. By using the time-domain smoothing technique, pressure waveforms which closely matched direct observations were obtained for both the single-cylinder diesel engine and the six-cylinder

diesel engine [60]. The estimated transform function (TF) may exhibit a phase hop of two octaves around the peak due to a divergence in the original frequency range caused by the time-domain smoothing method, which may substitute one peak for one valley.

When compared to cepstral smoothing (CS), exponentially windowing the time signal to move the transform line to the right of the frequency axis in the s-plane reduces the general level of the time signal, thus reducing its "valid scaling factor". Ghamry et al [61] achieved a more dependable cylinder pressure reconstruction by combining cepstral analysis with the advantage of acoustic emission's (AE) relative noise immunity. Although the pressure waveform was modelled and rebuilt using raw AE signals, the pressure rise during compression could not be precisely captured.

To tackle this issue, the signal was separated into two sections: the compression portion was reconstructed by polynomial fitting, while the injection/expansion portion was reconstructed using an autoregressive technique. Badawi et al. used inverse filtering to reconstruct cylinder pressure from measured engine vibrations and acoustics under similar conditions [62]. Fig. 9 is a schematic explanation of the inverse filtering technique. This technique, which is indirect, easy to use and low-cost, demonstrated good accuracy. Root mean square error (RMSE) percentages ranged from 2.4 % to 3.8 % compared to the measured cylinder pressure due to the non-linearity of the engine.

Han et al. [22] introduces an innovative recursive technique for estimating cylinder pressure using the Kalman filter, with engine structural vibration signals as input. The mean estimation error of the pressure peak (PP) ranges from −17.74 % to 12.00 %, with the majority of absolute values being below 6 %. The standard deviation (SD) of the PP error is predominantly below 1.10 %, signifying the estimatioń s stability. The absolute values of the mean pressure peak location (LPP) error do not surpass 2.30° CAD across all operational locations, with the associated standard deviation values being minimal, except for the test point at 2100 rpm and 60 N·m. This indicates that the suggested framework is highly effective for LPP estimation. The estimation results align with the coherence analysis, demonstrating superior performance at elevated engine speeds (e.g., 3000 rpm) relative to lower speeds (e.g., 1200 rpm). The employed linear time-invariant model is inappropriate for low-speed circumstances. Assuming an ideal linear time-invariant model between cylinder pressure and engine vibration signals enhances estimation results, yielding a PP error mean of 0.93–5.10 % and an LPP error mean of 0.64–1.86 CAD.

Antoni et al. [51] presented a basic methodology based on angular sampling and cyclic signal processing to design diagnostic indicators that are synchronised with the engine kinematics. It uses the presumption that the vibration signals are *cyclo*-stationary processes. This method seeks to address the challenge of distinguishing the many vibration sources' contributions, which frequently overlap because of the fleeting nature of the signals. The study demonstrates that the ideal inverse filter for reconstructing pressure varies on a regular basis and it offers recommendations for the efficient use of the deconvolution technique. It shows that the suggested methodology works with real vibration signals from a small diesel engine [52]. However, the inverse input–output relationship varies periodically only under specific circumstances, such as the existence of *cyclo*-stationary additive noise or structural variability in the input–output connection. The inverse filter might be invariant if these requirements are not satisfied. In practice, cycle-averaging can be difficult, particularly when dealing with non-stationary engine operating circumstances, as it is necessary to estimate the necessary statistics (such as covariance matrices) for the inverse filter identification.

Utilising vibration signals, Zurita et al. [63] employed multivariate data analysis (MVDA) techniques such as principal component analysis (PCA) and partial least squares (PLS) to reconstruct the cylinder pressure of a diesel engine. Three separate clusters representing various engine loads are identified by PCA, which assesses the underlying complexity of the vibration response and cylinder pressure data. PLS, on the other hand, reconstructs the cylinder pressure from vibration measurements and forecasts noise and exhaust emissions. It is challenging to create precise models because the vibration response signal used for the analysis is tainted by interference from a variety of sources, including impacting valves, piston slaps and combustion in nearby cylinders. The models' relatively low predictability and low degree of explanation in the X matrix were demonstrated by the results, which were probably caused by difficulties in processing the noisy vibration data. Further research on more statistically independent data acquired at separate periods is required to increase the resilience of the models, as the data used for their establishment and evaluation was recorded on the same occasion.

Neural network analysis (NNA) is a widely used technique that has demonstrated great capacity in modelling general input and output interactions, particularly in complex tasks [64]. The neural network is made up of an input layer with one neuron for each input, an output layer with one neuron for each output, and one or more hidden layers of neurons. Fig. 10 shows a representative example [65].

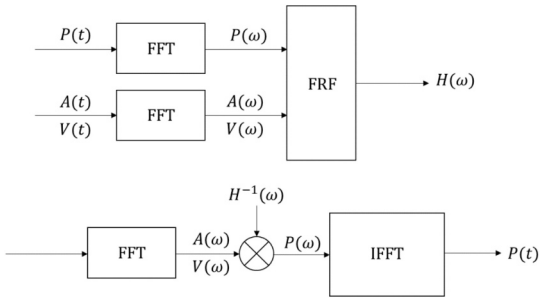

Fig. 9. Inverse filtering technique.

A subset of multilayer feedforward neural networks is the radial basis functions (RBF) network. A benefit of RBF networks over neural networks developed with the back-propagation technique is that the former can be learned more easily [66]. Since computational power is no longer a barrier to the application of sophisticated numerical techniques, black-box models have become increasingly prevalent. Du et al. [64] used generalized regression neural network (GRNN), one of the radial basis networks, to create a non-parametric mapping model between the engine cylinder head vibration signal frequency series and the cylinder pressure time series. The centres of the RBF network were chosen using the fuzzy c-means clustering approach, and the output layer weights are trained using the gradient descent methodology. Peña and Zurita [65] analysed the data by means of a thorough pre-processing procedure to minimise noise before sending them into a GRNN to predict cylinder pressure. In this case, the velocity rather than the acceleration signal, was used as the input data, and the response data was the cylinder pressure that had been filtered using a zero-phase digital filter. The results showed high accuracy, with the standard deviation of the maximum cylinder pressures varying between 0.03 and 1.01 %, outperforming other methods like the cepstrum method and multivariate data analysis. Roger [66] took Fourier transforms of both engine structure vibration and crankshaft speed fluctuation as input, which reduced the amount of data and selected the interesting frequencies for each measurement method. The root-mean-square (RMS) errors for the validation set were as follows: 3.5 bars (3.4 % of measured values) for predicted maximum pressure; 1.5 CAD for the predicted location of maximum pressure; 2.6 bars/CAD for the predicted maximum rate of pressure rise; 0.9 CAD for the predicted location of maximum rate of pressure rise; and 0.7 bar for the indicated mean effective pressure (IMEP) from the predicted pressure waveform. Bizon and Continillo [24] applied the original vibration signal at the unprocessed ± 30 CAD around top dead centre as input. They demonstrated good accuracy in reconstructing the in-cylinder pressure signal and predicting key parameters such as pressure peak value and location, as well as MBF50 location, across multiple engine operating conditions.

Taking the input from an affordable accelerometer mounted on the engine block, Bizon et al. [67] constructed reliable and effective artificial neural networks (ANNs) to reconstruct the in-cylinder pressure of diesel engines in defined engine conditions. Time series from in-cylinder pressure signals and vibration signals recorded on a cylinder far from the one where the pressure is measured were employed to train the RBF network. The largest RMSE peak cylinder pressure location was 0.956 CAD; the highest RMSE of the pressure peak value was 3.896 %; and the RMSE of the MBF50 site was 1.649 CAD.

Moreover, Nguyen et al. [25] showcased the effectiveness and precision of pressure curve reconstruction by the application of RBF and GRNN with an HCCI engine. Only the original vibration signal at the unprocessed ± 40 CAD around top dead centre was taken as input to reduce the computational time. The approach was validated with both low- and high-load operating points, and the GRNN model was found to perform better than the RBF model in this case. To improve accuracy, Trimby et al. [68] implement the Levenberg-Marquardt algorithm (LMA) to develop a new approach using time-delay feedforward artificial neural networks. In this paper, both time-delayed values and future values of a single input variable, such as crank kinematics or engine block vibration acceleration measurements, were the input for the reconstruction of in-cylinder pressure. As a result, the model was able to accurately represent the whole combustion process, including the data surrounding top dead centre (TDC), which is usually where the cylinder pressure peaks are located. This mitigates the information loss that could arise from relying solely on past data because of connecting rod inertia. However, for the engine block vibration-based cylinder pressure reconstruction, the RMSE of pressure curve was between 1.32 % and 4.33 %; the RMSE of normalised peak pressure was between 2.99 % and 14.1 %; and the RMSE of the peak pressure position was between 0.91 and 5.01 CAD, so the margin of error is rather large.

Several researchers have adopted a direct approach by using raw cylinder pressure measurements as inputs to predict pressure characteristics across varying operating conditions. Song et al. [69] developed a hybrid PCA-ANN algorithm for cylinder pressure reconstruction which accounts for crankshaft flexibility – a key factor in combustion measurement inaccuracies. Their method achieved pressure curve reconstruction with RMSE values of 0.4–0.6 bar, peak pressure errors below 0.04 bar, and peak pressure location deviations under 2 CAD. The model also demonstrated strong performance in estimating IMEP (RMSE $<$ 0.3 bar) and CA50 (RMSE $<$ 0.5 CAD). However, the study notes two important limitations. First, the approach struggles to capture nonlinear cycle-to-cycle pressure variations critical for detecting misfires, knocking and other abnormal combustion events. Second, while PCA effectively reduces the input dimensions from 17 to 6, the resulting feature transformations lose physical interpretability, complicating combustion behaviour analysis through network weights. In a complementary study, Ricci et al. [70] implemented a back-propagation ANN (BPANN) for cylinder pressure prediction, achieving remarkable consistency with RMSE values below 0.44 % and peak pressure timing errors under 5 % across diverse operating conditions. Benchmarked against GT-Power simulations (RMSE: 0.92–1.57 %), the ANN approach demonstrated superior computational efficiency while maintaining – and in some cases improving – prediction accuracy. This comparison highlights ANNs' dual advantage in combustion analysis: substantially reduced computation time coupled

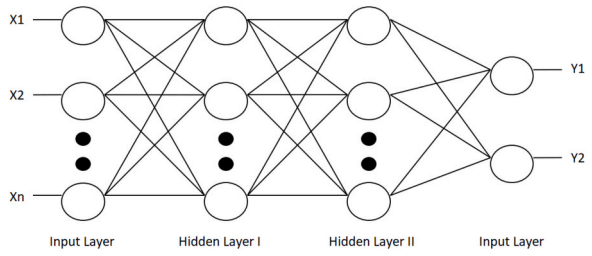

Fig. 10. Neural network.

with enhanced precision.

Table 7 summarises the various methods for reconstructing cylinder pressure curves, including cepstral analysis, inverse filtering, time-domain smoothing, recursive estimation algorithms and neural network analysis. Most studies focused on CI engines operating at a variety of engine speeds and loads. SI engines were also studied, particularly in free slow acceleration conditions, while the only study on an HCCI engine was published relatively recently, in 2022. The complete pressure curves were estimated and validated by different metrics and methods, such as overall comparison, reconstruction error percentage and root mean square error of peak pressure.

Cepstral analysis and inverse filtering were among the earliest used methods for reconstructing cylinder pressure curves. They involve transforming the vibration signals into a different domain (cepstrum) and then applying inverse filtering to reconstruct the

Table 7
Summary of cylinder pressure curve reconstruction.

Ref.	Year	Engine Type	Operating conditions	Vibration sensor	Analytical approach	Error, remarks
[54]	1986	CI, 6-cylinder, 350 horsepower	1800 & 2100 rpm, full load	Accelerometer	Cepstral analysis and multi-channel inverse filtering	Complete pressure curve, excellent for the 1800 RPM
[58]	1997	SI, 4-cylinder, 1300 cm^3	3100–5000 rpm; free slow acceleration	Accelerometer	Determination of frequency response function, inverse filtering	Indicated pressure waveforms, Peak pressure: 4 % (mean error)
[59]	1999	CI, 1-cylinder	2400—3600 rpm, full load	Accelerometer	Time-domain smoothing (TDS) and cepstral smoothing (CS) procedure	Complete pressure curve, match better with smoothing operations
[61]	2004	CI, 4-cylinder, 102 bhp (Brake HorsePower)	750–1650 rpm, 30 Nm load	Acoustic Emssion	Inverse filtering with complex cepstrum analysis	Complete pressure curve: less than 7 % (reconstruction error percentage)
[62]	2006	CI, 1-cylinder, 511 cm^3	700 rpm; 0 %, 40 % and 90 % of full load	Accelerometer B&K 4367, Microphone B&K 4190	Inverse filter	Complete pressure curve: 2.6 % (0 load), 2.4 % (40 load), 3.8 % (full load)
[22]	2018	CI, 4-cylinder, 2000 cm^3	1200–3000 rpm, 0.38–1.13 MPa (BMEP)	Accelerometer	Recursive estimation algorithm based on Kalman filter	Peak pressure: 4.5 % (mean error), location of peak pressure: 1.9 CAD (mean error)
[52]	2002	CI, 4-cylinder, 1905 cm^3	900 rpm	Accelerometer	Inverse filtering with periodically variable filters	Complete pressure curve
[63]	2004	CI, 6-cylinder, 11000 cm^3	800–2000; 10 %- 100 % of full load	Accelerometer PCB 353 M15, 1–10000 Hz	Multivariate data analysis for peak pressure prediction and partial least squares model for pressure reconstruction	Peak pressure: 5 % @ 800 rpm, 39 % @2000 rpm (mean error)
[64]	2011	CI, 2-cylinder, 2003.9 cm^3	900–1500 rpm, 80 kW load	Accelerometer	GRNN, input data: frequency characteristics of the engine cylinder head vibration signals	Peak pressure
[65]	2005	CI, 1-cylinder, 522 cm^3	800–2000 rpm; 10 %-100 % of full load	Accelerometer PCB 353 M15, 1–10000 Hz	GRNN, input data: velocity	Peak pressure: 1 % (difference in STD)
[66]	2006	CI, 6-cylinder 11000 cm^3	800–2000 rpm; 10 % −90 % of full load	Accelerometer PCB 353 M15, 1–10000 Hz	RBF-ANN, input data: Fourier transforms of acceleration and crankshaft speed	Peak pressure: 3.4 % (RMSE), location of peak pressure: 6 CAD (RMSE), PRR: 0.26MPA/CAD (RMSE)
[24]	2011	CI, 1-cylinder, 522 cm^3	1000–2000 rpm, 1.01–1.34 bar (intake pressure)	Accelerometer	RBF, input data: signal from a low-cost accelerometer	Peak pressure: 2.7 % (RMSE), Peak location: 1.45 % (RMSE), MBF50: 3.41 % (RMSE)
[67]	2013	CI, 3-cylinder, 1028 cm^3	1800–3400 rpm; idle run	Accelerometer, up to 1.5 kHz	RBF-ANN	Peak pressure: 3.9 % (RMSE), CA50: 1.6 CAD (RMSE)
[25]	2022	HCCI, 1-cylinder, 499 cm^3	900–2300 rpm; 0.16–0.45 Mpa;(IMEP)	Accelerometer PCB ICP M338A34, 0.7–3000 Hz	ANN (RBF, GRN)	Complete pressure curve: 0.19 MPa (RMSE); peak pressure: 0.08 MPa (RMSE); peak pressure location: 4.5 CAD (RMSE)
[68]	2017	SI, 3-cylinder, 1125 cm^3	1000–2000 rpm; 0.11–0.34 MPa (BMEP)	Acceleration-type knock sensor	ANN (time-delay feedforward) with LMA	Complete pressure curve: 4.3 % (RMSE), normalized peak pressure: 4.3 % (RMSE), peak pressure position: 5.01CAD (RMSE)
[69]	2024	CI, 6-cylinder turbocharged, 1294 cm^3	800–1700 rpm; 0–900 load torque (N·m)	N/A	PCA, ANN (single-layer feed-forward perceptron)	Complete pressure curve: 0.4–0.6 bar (RMSE); Peak pressure $<$ 0.04 bar (RMSE); Peak pressure timing: $<$ 2 CAD (RMSE); IMEP $<$ 0.3 bar (RMSE); CA50 $<$ 0.5 CAD (RMSE)
[70]	2025	SI, 1-cylinder, 500 cm^3	1000 rpm; λ 1.6, 2.0, and 2.3; Ignition Timing −1CAD to −19CAD after TDC	N/A	GT-POWER and BPANN	Complete pressure curve: 0.44 % (RMSE); Peak pressure timing: $<$ 5 % (RMSE)

pressure curve. These methods showed good accuracy, particularly at low engine speeds, but their performance could vary with different engine types and operating conditions. For example, the reconstruction error percentage was less than 7 % for a four-cylinder CI engine at under 750 rpm, but less than 3.8 % for single-cylinder CI engine at under 700 rpm. Time-domain smoothing and cepstral smoothing involve smoothing the vibration signals in the time domain to reduce noise and improve the match of the reconstructed pressure curve with the measured one. They provided better results than other methods, especially when dealing with noisy data. The Kalman filter-based approach is a recursive algorithm that estimates the state of a dynamic system from a series of noisy measurements. It demonstrated high accuracy in estimating peak pressure (mean error of 4.5 %) and its location (mean error of 1.9 CAD), making it suitable for real-time applications. Multivariate data analysis such as PCA and PLS analyses the relationship between multiple variables (e.g., vibration signals and cylinder pressure) to reconstruct the pressure curve. They successfully reconstructed cylinder pressures with peak pressure errors ranging from 5 % to 39 %, depending on the engine's speed. Neural networks, including GRNN and RBF networks, are advanced machine learning models that can learn complex relationships between input and output data. They showed high accuracy in predicting peak pressure with errors as low as 1 % for a single-cylinder CI engine at under 2000 rpm and full load. CA50 was predicted with errors as low as 1.6 CAD for a three-cylinder CI engine at under 3400 rpm. CA50 describes the crank angle at which 50 % of the heat from combustion has been released. These methods also show good accuracy in HCCI engine with RMSE of complete curve 0.19 MPa, peak pressure 0.08 MPa and peak pressure location 4.5 CAD. The Levenberg-Marquardt algorithm (LMA) uses time-delay feedforward neural networks to accurately represent the entire combustion process, including data around top dead centre (TDC). However, the margin of error was relatively large in some cases, with RMSEs ranging from 1.32 % to 14.1 %.

Neural network analysis and recursive estimation algorithms generally provided the highest accuracy, with low error margins in predicting peak pressure and its location, demonstrating broader applicability across different engine types and operating conditions. Cepstral analysis and inverse filtering also showed good accuracy, particularly at low engine speed. Time-domain smoothing and cepstral smoothing improved the match of predicted pressure curves with the measured curves by reducing noise.

2.2.2. Analysis of combustion-induced pressure oscillations

In addition to the overall pressure evolution, the combustion process within an internal-combustion engine exhibits distinct pressure oscillations that reflect the high-frequency dynamics of heat release and acoustic resonance in the combustion chamber.

Knocking, or pressure oscillation, tends to occur easily in SI gasoline engines operating with a high compression ratio. In such engines, combustion follows a homogeneous premixed pattern. When the air–fuel mixture is ignited by the spark plug, flame propagation begins from the ignition centre. However, under certain conditions, portions of the unburned mixture self-ignite due to elevated temperatures or be triggered by localized hot spots [71]. This results in a rapid increase in both temperature and pressure, generating the propagation and reflection of pressure waves within the combustion chamber [72]. This is why knocking happens. This phenomenon has negative impact on power performance, fuel economy and reliability of gasoline engine. Ideally, combustion should happen right at the point that the engine is about to knock or not knock. Therefore, extensive research has been devoted to understanding and mitigating knock in gasoline engines. Stefano et al. [73] examined the knock resistance of gasoline–propane blends and developed a calibrated knock onset prediction sub-model suitable for integration into zero-dimensional thermodynamic models commonly used for engine performance optimization. Assuming the contents of combustion chamber are homogeneous, Tougri et al. [74] developed a zero-dimensional thermodynamic model for estimating the onset of the knocking phenomena in a flex-fuel engine using gasohol (gasoline blended with anhydrous ethanol) and blends of gasohol with hydrous ethanol.

Regarding compression ignition diesel engines, combustion typically occurs in a diffusion-dominated mode, where premixed combustion governs the initial reaction processes. During the first stage of combustion, various regions of the air–fuel mixture auto-ignite, and flame fronts propagate as pressure waves travel through the chamber. When these waves encounter the combustion chamber walls, they reflect and interact, producing high-frequency pressure oscillations within the gas. The resonance frequency of these oscillations depends on the geometry of the combustion chamber and the speed of sound in the mixture—both influenced by thermodynamic parameters such as temperature, pressure, and density [75]. The intensity of oscillations is closely related to the pressure gradient that develops in the early combustion phase, which in turn depends on key combustion characteristics such as the extent of premixed combustion and the ignition delay (ID) [76]. Zhang et al. [53] applied Acoustic Gas Source Tomography (AGST) to analyze in-cylinder pressure oscillations in a multi-injection direct-injection (DI) diesel engine under varying operating and injection conditions. Their results revealed that, in DI diesel engines employing a pilot–main injection strategy, the pilot injection stage generates the highest pressure oscillation amplitude and energy. Moreover, as engine speed and load increase, pressure oscillations intensify; however, they tend to weaken at 2200 r/min, primarily due to the influence of injection parameters. Similarly, Zheng et al. [50] utilized time-varying filter-based empirical mode decomposition to extract high-frequency oscillation components. They examined the effects of engine speed, load, rail pressure, main injection timing, pilot injection interval, and pilot injection quantity on pressure oscillations. The results showed that the energy of high-frequency oscillations peaks at medium-to-high engine speeds and increases with both load and rail pressure. However, the relationship between high-frequency oscillation energy and fuel injection parameters was found to be non-monotonic.

Characterizing pressure oscillations is a vital enhancement of in-cylinder pressure analysis, connecting the disparity between macroscopic combustion pressure changes and microscopic auditory events. Their precise identification not only improves vibration-based combustion diagnostics but also facilitates the early detection of anomalous combustion events and the enhancement of combustion noise prediction models.

3. Combustion-induced vibration

Filtering, EMD, and VMD techniques are commonly used to isolate combustion noise from other engine vibrations. Among them, VMD shows strong potential for real-time use, especially when paired with machine learning.

3.1. Filtering technologies

Filtering technology plays a crucial role in engine noise decomposition, because it helps isolate and analyse specific frequency components or noise sources in the acoustic signals generated by internal combustion engines. Various filtering techniques are employed to enhance the accuracy of noise analysis.

Frequency-based filters separate engine noise into specific bands associated with different sources, such as combustion, piston slap, gears, valve knock, and the fuel pump. These distinct frequency characteristics enable targeted extraction in the frequency domain. This method often employs fast Fourier transform (FFT) to convert the time-domain signal into the frequency domain. The frequency-based filters including low-pass filters (LPF) [68], high-pass filters (HPF) [42] and band-pass filters (BPF) [39] are then applied to isolate specific frequency ranges corresponding to various engine components or phenomena. For instance, combustion source at distinct frequency ranges can be identified within the vibration signals. Additionally, Jung et al. [77] devised a band-pass filter spanning 600–900 Hz specifically tailored to extract combustion-related information from vibration signals.

Several advanced filters have been designed based on engine operating conditions and the *cyclo*-stationary nature of ICE signals, including the cyclic Wiener filter (CWF) [22]. In CWF, the impulse response G(t) can be estimated using the in-cylinder pressure P(t) as a reference. Assuming statistical uncorrelation between thermal and mechanical vibration sources, the thermal contributions – specifically, combustion noise-induced vibration $\tilde{x}_{th}(t)$ – can be derived through the convolution of the input P(t) and the impulse response G(t). Then the mechanical contribution $\tilde{x}_{me}(t)$ is obtained by simple subtraction of $\tilde{x}_{th}(t)$ fromthe measured vibration signals, as shown in Fig. 11.

Pruvost et al. [78] simplified separation by using enhanced separation filters (ESF) in diesel engines. These filters isolate combustion and mechanical noise by focusing on the random signal components and applying asymmetric Tukey windows (ATW). Antoni et al. [79] expanded this framework to account for transient speed conditions, such as engine run-up, introducing challenges beyond the typical *cyclo*-stationary assumptions. First, the concept of *cyclo*-non-stationarity replaces the assumption of *cyclo*-stationarity. Second, conventional cyclic averaging is re-evaluated. Third, separation filter design explicitly accounts for speed dependence. In this approach, a cyclic difference operator replaces traditional cyclic averaging. Speed dependence is handled using a flexible B-spline basis, with knot density automatically adjusted based on the data. The proposed separation filters (SFs) are straightforward yet robust, tailored to differentiate combustion noise signals based on various speed and load conditions.

Table 8 summarises the various filter technologies in the reviewed studies, where ICP represents in-cylinder pressure; VS represent vibration signal; and EN represents engine noise. These filter technologies allow engineers to isolate and identify various noise sources within engines, which contributes to developing targeted noise reduction strategies to enhance engine performance and reduce overall noise emissions. Custom separation filters must be designed for different operating conditions, allowing precise identification of vibration and noise sources. However, the complexity of the filter model somewhat limits its applicability as a filtering method.

3.2. Empirical mode decomposition technologies

Empirical mode decomposition (EMD) is a signal processing method which breaks down a complex signal into intrinsic mode functions (IMFs) and a residual, based on its local time-scale characteristics.

$$x(t) = \sum_{i=1}^{N} imf_i(t) + r(\mathrm{t}) \tag{1}$$

where $imf_i(t)$ is the i-th intrinsic mode function.

EMD is a mature and widely established technique for adaptive decomposition of non-linear and non-stationary signals into IMFs. The algorithm iteratively extracts oscillatory components by removing local mean trends computed from upper and lower envelopes of

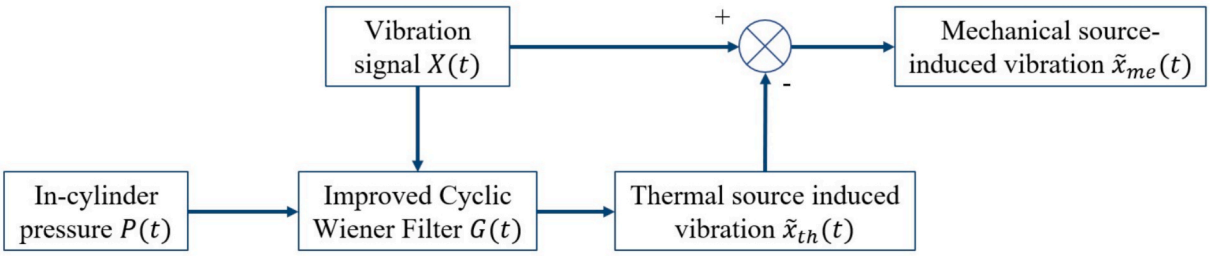

Fig. 11. Principle of cyclic Wiener filter for separation.

Table 8
Comparison of various filter technologies.

Engine type	Input signal	Analytical approach	Output signal	Application	Validation	Ref.
SI, 3-cyl.	ICP, VS	Time-delay neural network, LPF,	ICP	ICP reconstruction from VS	Reconstruction accuracy of synchronous data	[68]
CI, 1-cyl.	ICP, VS	HPF, S transform	Combustion parameters	Identification combustion parameters from VS	Reconstruction in successive cycle	[42]
CI, 3-cyl.	ICP, VS	BPF	Combustion parameters	Estimation of combustion parameters from VS	The square value of the correlation coefficient	[39]
CI, 4-cyl.	ICP, VS	WT, BPF	Combustion factors	Prediction of combustion characteristics for EN control	Accuracy of correlation	[77]
CI, 4-cyl.	ICP, VS	CWF	Combustion noise	Separation of combustion noise	Analysis by experience	[80]
CI, 4-cyl.	ICP, VS	ESF	Combustion noise	Separation of combustion noise	Validation by simulation results	[78]
CI, 4-cyl.	EN, VS, ICP	SF, HPF	Combustion noise	Separation of combustion noise incorporating speed dependence	95 % confidence interval	[79]

the signal. This process, known as shifting, continues until a component satisfies the IMF conditions. Fig. 12 is a schematic representation of this iterative procedure.

This adaptability to non-stationary and nonlinear signals makes EMD particularly suitable for engine noise separation. EMD́s iterative nature ensures that each IMF represents a distinct frequency component of the signal. For example, Bi et al. [27] introduced a technique for identifying engine knock characteristics in gasoline engines using vibration signal analysis. The technique integrates wavelet denoising and EMD to accurately discern knock features, such as light knock, from vibration signals. Wavelet denoising removes unrelated high-frequency noise, while EMD extracts knock-related features more clearly, as shown in Fig. 13. The IMF1 component in Fig. 13(a) shows two distinct effects corresponding to knock events at approximately 0.005 s and 0.016 s. Fig. 13(b) shows that the energy is mostly concentrated in the 6–10 kHz range, aligning with the characteristic knock resonance of 7–8 kHz. This method reduces computation time while still reliably detecting knock, outperforming current techniques. This studýs principal outcomes are the capability to isolate knock characteristics from other vibration sources, distinguish knock from standard combustion and achieve rapid and dependable knock detection.

However, modal aliasing significantly reduces the precision of the EMD method and can produce incorrect IMF components [81]. The presence of overlapping signal elements complicates time–frequency analysis, resulting in disordered outputs due to scattered signal distributions. This complexity makes it challenging to intuitively analyse the outcomes. Wu et al. [30] addressed this issue by incorporating the noise-assisted signal analysis method into the EMD theory, introducing the concept of ensemble empirical mode decomposition (EEMD). This novel approach significantly mitigated the issue of modal mixing, thereby substantially enhancing the accuracy of signal mode decomposition. Bi et al. [14] used ensemble empirical mode decomposition along with robust independent component analysis techniques to isolate and identify combustion noise, piston knocking noise, and exhaust noise from the noise generated by gasoline engines.

Although the EEMD method resolves mode-mixing, selecting parameters like noise amplitude and ensemble size is challenging and critically affects decomposition accuracy. EEMD also has a high computational cost.

Li et al. [82] proposed time varying filter-based empirical mode decomposition (TVF-EMD), a method which addresses signal separation challenges and reduces inconsistencies in decomposition. This approach demonstrates superior decomposition performance compared with the traditional EMD method. TVF-EMD, characterised as a data-driven adaptive decomposition technique, has been applied in various fields, including bearing fault diagnosis [83] machinery fault-finding [81], wind speed forecasting [84] and modal

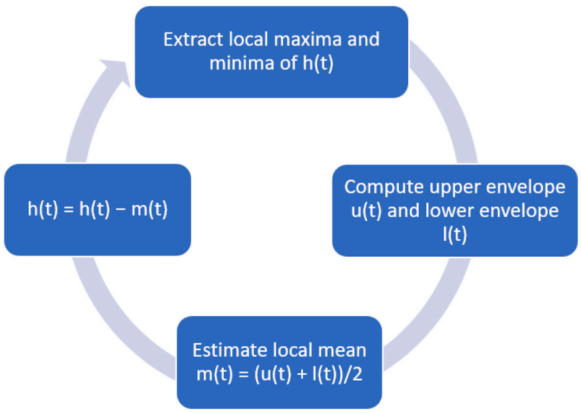

Fig. 12. EMD shifting processing.

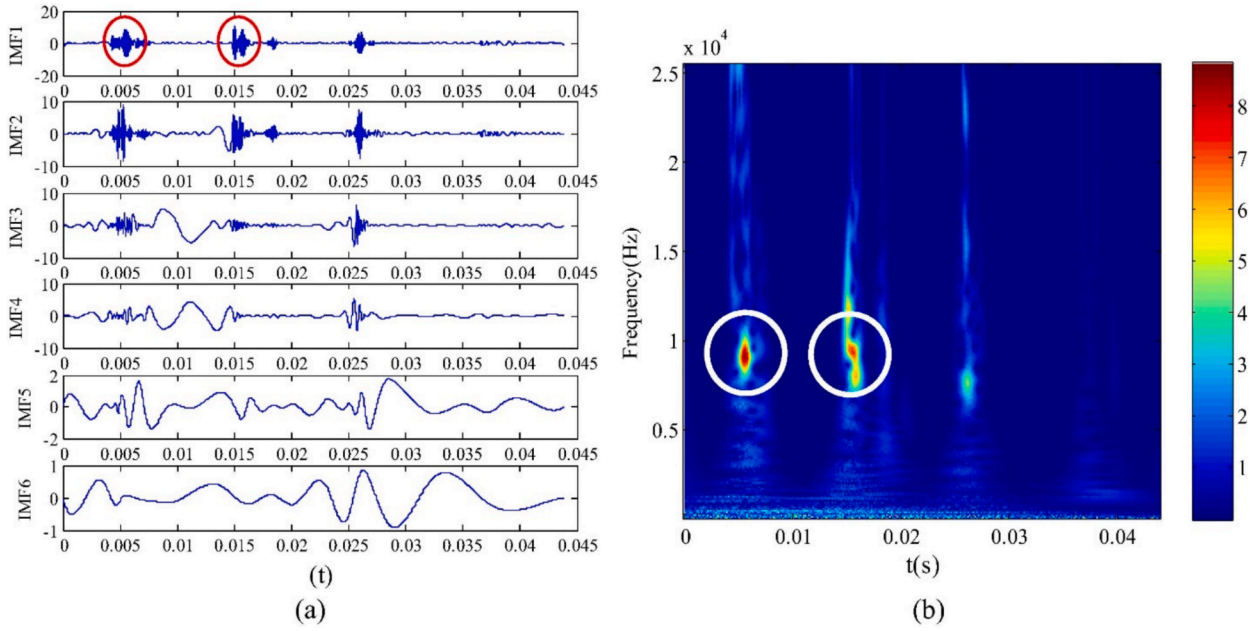

Fig. 13. EMD decomposition results of the wavelet denoised signal for the condition measured from cylinder 4: (a) EMD result for the wavelet denoised signal; (b) time–frequency spectrogram of the IMF1 component [27]. (Reproduced from Mechanical Systems and Signal Processing with permission from Elsevier).

identification [85]. In particular, Yao et al. [86] utilized TVF-EMD in conjunction with RobustICA to identify combustion noise and piston slap noise from a single-channel noise signal in a diesel engine.

Table 9 summarises the EMD technologies for IC engines. EEMD and TVF-EMD address some of the limitations of traditional EMD, offering improved robustness and adaptability to varying signal conditions. Advances in these decomposition techniques have significantly contributed to signal processing applications, ranging from biomedical signal analysis to mechanical vibration diagnostics. Future research may focus on further refining these methods, optimising computational efficiency, and exploring their integration with emerging technologies, such as machine learning, for enhanced signal analysis and interpretation.

3.3. *Variational mode decomposition technologies*

VMD aims to decompose a real-valued signal into distinct sub-signals (modes), each with defined sparsity characteristics. These modes collectively preserve the original signal's key features. VMD integrates techniques such as Wiener filtering, Hilbert transforms, and alternating direction multiplier method (ADMM) to achieve decomposition [28]. The mathematical model is expressed as follows:

$$\min_{\{u_k\},\{\omega_k\}} \left\{ \sum_k \left\| \partial_t \left[\left(\delta(t) + \frac{j}{\pi t} \right) * u_k(t) \right] e^{-j\omega_k t} \right\|_2^2 \right\} \tag{2}$$

$$s.t. \sum_k u_k = x \tag{3}$$

where, $\{u_k\}$ represents the set of modal signals $\{u_1, \cdots, u_k\}$, and $\{\omega_k\}$ represents the set of centre frequencies $\{\omega_1, \cdots, \omega_k\}$. The variable x represents the original signal, δ denotes the Dirac delta function, and $\sum_k := \sum_{k=1}^{k}$, represents the summation notation over the range

Table 9
Comparison of various EMD technologies for IC engines.

Engine type	Input signal	Analytical approach	Output signal	Application	Validation	Ref.
SI, 4-cyl.	VS	EMD, wavelet-denoising	Knock components of combustion	Separation and detection of combustion knock	CWT, EEMD	[27]
SI, 4-cyl.	EN	EEMD, RobustICA	Noise components of exhaust, combustion and piston slap	Separation of various noise source	Semi-anechoic laboratory, CWT	[14]
CI, 6-cyl.	EN	TVF-EMD, RobustICA	Noise components of combustion and piston slap	Separation of noise source	CWT, FFT, CWF and dynamic model	[86]

of k from 1 to K.

Unlike other methods, VMD avoids assuming mode orthogonality, enabling more flexible and accurate signal decomposition. The variational approach provides robustness to noise and non-stationary characteristics inherent in engine noise. For instance, Yao et al. [16] utilised VMD technology in conjunction with RobustICA to distinguish combustion noise and piston slap noise in a diesel engine operating at low speeds. Fig. 14 depicts their noise source identification system: step 2 shows how the single-channel noise signal is decomposed into multiple IMFs using VMD. Researchers analysed the correlation between each IMF and the measured signal to identify those most related to the engine source. The selected IMFs were utilized as input in step 3 to ensure maximum independence among all the IMFs.

Fig. 15 illustrates how CWT enabled identification of noise components from combustion and piston slap. It shows that the frequency of the IC1 component is concentrated at 3700 Hz. The IC1 time-domain waveform shows a significant amplitude change near 370 CAD. Fig. 15(c) shows that cylinder 6 produces more energy, likely because cylinders 1–5 were shielded with lead masks. 370 CAD is the ignition angle of the number 6 cylinder in a diesel engine with an ignition sequence of 1–5–3–6–4. Therefore, the IC1 component can be attributed to combustion and identified as combustion noise. A comparable method may be employed to detect the noise originating from an alternative source. A comparison of the VMD-RobustICA-CWT method and the EEMD-RobustICA-CWT method shows that the former yields more accurate and pure noise signals, with reduced interference.

Under high-speed conditions, Yao et al. [17] incorporated a binaural sound localisation method (BSLM) to enhance the effectiveness of the proposed decomposition technology. Zhang et al. [87] introduced an integrated VMD-PCA-FAHP approach to identify and rank six primary noise sources in a diesel engine. The results indicate the following descending order of influence: oil pan, left block, valve cover, flywheel housing, and right block. The validation is primarily based on controlled rig tests conducted on a specific diesel engine model, so the findings may have limited significance to real-world operating conditions or other engine configurations. Sun et al. [88] introduced a knock recognition method that relies on the combination of wavelet transform and the variational mode decomposition algorithm. This approach is employed to process the knock sensor signal and extract pertinent knock features.

The accuracy and efficiency of the VMD strongly depend on the parameters pre-set manually, thereby constraining the adaptability of the method. A significant deviation in the chosen mode number can lead to the exclusion or blending of modes. Consequently, a technique known as adaptive variational mode decomposition (AVMD) [89] has been introduced to autonomously ascertain the mode number, leveraging the characteristics of intrinsic mode functions. Meanwhile, the penalty factor α – another critical present parameter influencing IMF frequency bandwidth – has received comparatively less attention. Although Pu et al. [90] proposed separate optimisation approaches for K and α, the interdependent relationship between IMF quantity and bandwidth remains unaddressed. Furthermore, this optimisation process is susceptible to convergence at local optima, as noted by Yi et al. [91]. Zheng et al. [92] developed a dichotomy-based VMD method that can automatically identify the centre frequency of actual signal components without pre-set rules. This gets rid of the need to manually choose decomposition parameters in the traditional VMD algorithm. Employing this approach, they [93] extracted the vibration signal characterizing abnormal noise. Results indicated that the idling abnormal noise was caused by the impact of the rotor and stator inside the camshaft phaser of the variable camshaft timing system.

Fuzzy distribution entropy (FuzzDistEn) combines the empirical probability density function from distribution entropy (DistEn) with the fuzzy membership function of fuzzy entropy (FuzzEn), ensuring accurate and effective assessment of system complexity. However, due to the nonlinear and non-stationary nature of diesel engine noise signals, determining optimal VMD parameters using a single index remains challenging. To address this limitation, Zhou et al. [94] incorporated weighted FuzzDistEn into VMD parameter optimisation, thereby developing a parameter-adaptive VMD-PCA methodology. The proposed method effectively isolates five distinct surface-radiated noise sources in diesel engine noise identification, as validated through bench-scale experiments. These include oil pan noise (around 280 Hz); valve cover noise (around 770 Hz); fuel injection noise (around 1200 Hz); combustion noise (around 1500 Hz); and piston-slap noise (around 2120 Hz). The proposed method still struggles with computational intensity and guarantees of globally optimal solutions due to optimisation algorithms used to select parameters. Furthermore, the identification of specific noise sources is based on characteristic frequencies, which may vary under different operating conditions. This could limit the robustness of the method when applied to variable engine loads or different engine types.

Moreover, existing methods for signal decomposition and feature extraction exhibit noticeable deviations and high computational complexity when dealing with impact feature extraction. This is primarily due to the severe frequency aliasing in actual multi-impact signals and the complex nature of impact responses. To address this, Zhao et al. [95] conducted research on the time-domain decomposition of impact signals and introduced a variational time-domain decomposition (VTDD) method based on the VMD algorithm framework (using an augmented Lagrangian and ADMM). The VTDD separates a vibration signal $S(t) = \sum_{k=1}^{K} s_k(t)$ from reciprocating equipment into its individual impacts directly in the time domain by minimizing a high-order amplitude central moment – i.e., discovers the centre time t_k, time-extent (boundaries), and waveform of each impact, even when numerous impacts overlap and the spectrum is muddy. The constrained variational problem model is as follows:

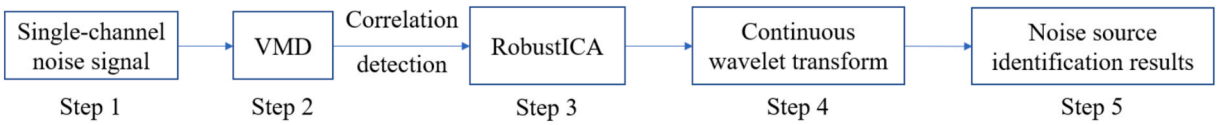

Fig. 14. Noise source identification flowchart [16]. (Redrawn from Applied Acoustics with permission from Elsevier).

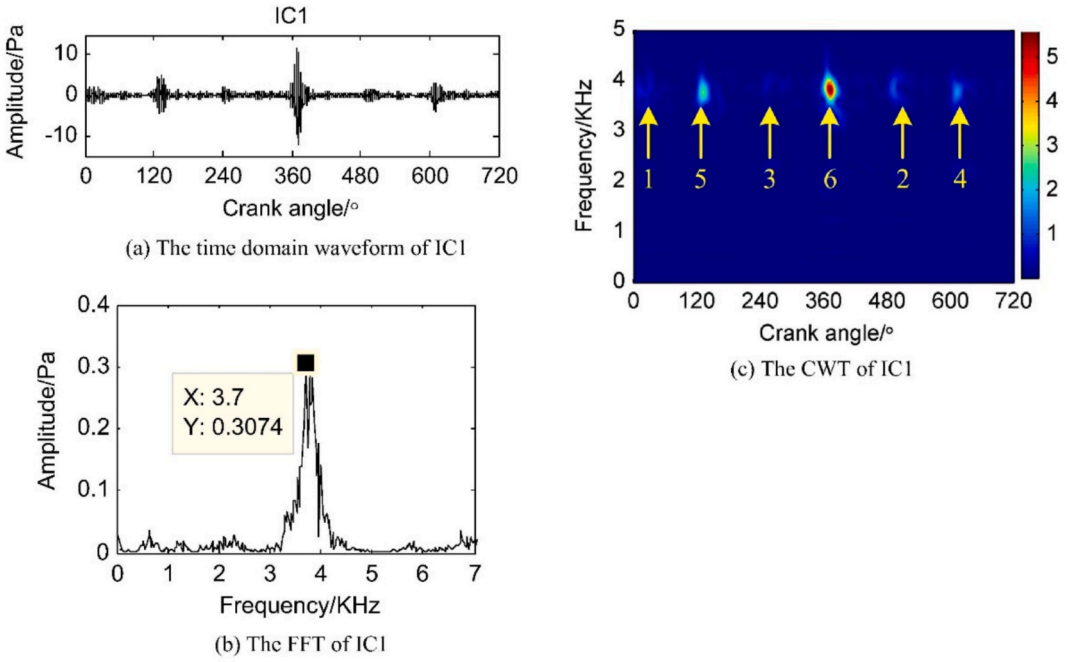

Fig. 15. The time domain waveform, FFT and CWT of IC1 by VMD-RobustICA-CWT method [16] (Reproduced from Mechanical Systems and Signal Processing with permission from Elsevier).

$$\min_{\{s_k\},\{t_k\}} \left\{ \sum_k \left\| (t - t_k)^p s_k(t) \right\|_2^2 \right\} \tag{4}$$

$$s.t. \sum_k s_k = S \tag{5}$$

where $\{s_k\} = \{s_1, \cdots, s_K\}$ represents the decomposed components, with $s_k(t)$ indicating the signal amplitude at time t; $\{t_k\} = \{t_1, \cdots, t_K\}$ denotes the temporal positions of all decomposed component centers, where $t \in [0, 1]$ signifies the normalized time of a signal. The exponential coefficient p is the order, defined as a non-zero natural number. K denotes the number of decompositions, and k is the sequence number corresponding to each decomposed component, where $\sum_k = \sum_{k=1}^{K} = 1$. S represents the original signal.

Each particle is forced to focus energy firmly about its centre in order to minimize that instant, which is what impacts naturally do. The order p determines how "boxy" the extraction window is; a higher p tightens the window, but if it is set too high, it may skew the predicted centre (they advise $p \in [1, 4]$). Besides, noise can be spurious impacts if K grows, which can be mitigated via interference/residual criteria.

Furthermore, Zhao et al. [31] proposed a novel variational time–frequency adaptive decomposition (VTFAD) method for extracting reciprocating mechanical impact features. Building on the VTDD, this method considers signal frequency characteristics and focuses on locating and extracting impact signals in the time–frequency domain. This approach significantly enhances the capability to identify new weak impact features in the early stages of faults. VTFAD demonstrates higher decomposition accuracy (cosine similarity 0.993 vs 0.960), lower computational complexity (45 s vs 115 s in simulation and 41 s vs 289 s in real data), and robustness to noise and

Table 10
Difference in the methods.

Method	Domain	Objective	Extracted Components	Parameter Adaptivity	Best Suited For
VMD	F*	Minimize bandwidth around ω_k	Narrowband AM–FM modes	Requires manual K and penalty	Signal decomposition based on frequency band energy
VTDD	T**	Minimize time-domain amplitude moments around t_k	Transient impacts localized in time	Automatic K, adaptive α_k, guided by decay model	Impact extraction based on time-domain impact energy and morphology
VTFAD	F-T***	Minimize spectral central moment in (t, ω)	Impact events localized in both time & frequency	Automatic K, adaptive α via spectral area	Impact extraction based on time–frequency energy

* Decomposition of the signal in the frequency domain.
** Decomposition of the signal in the time domain.
*** Decomposition of the signal in the time–frequency domain.

overlapping impacts (RMS error 7.5 % vs 9.2 %) than VMD + VTDD. Table 10 summarizes the differences and relationships among VMD, VTDD, and VTFAD.

In summation, emerges as a promising technique for ICE noise separation, due to its adaptability to non-stationary signals and inherent noise robustness. Table 11 summarises the VMD-based approaches and highlights how they enhance diagnostics and performance optimisation by decomposing complex noise signatures into interpretable components. However, several challenges persist:

- Dependence on parameter optimisation: While hierarchical structuring, weighted FuzzDistEn, and correlation analysis improve VMD's adaptability, the method remains reliant on computational optimisation for parameter selection. This process can be resource-intensive and may converge to suboptimal solutions
- Limited scope: Current implementations identify noise sources via characteristic frequencies, which may shift across operating conditions or engine types, reducing method robustness
- Non-order and non-stationary sources: although VMD handles non-order noise, its effectiveness diminishes when source frequencies overlap or lack well-defined signatures

Future work to address these limitations should focus on:

- Real-time implementation: optimising computational efficiency for on-board noise diagnosis and condition monitoring
- Multi-source analysis: extending VMD to disentangle overlapping noise sources in complex signal environments
- Machine-learning integration: leveraging deep learning for automated feature extraction and classification to complement decomposition
- Multi-modal data fusion: augmenting acoustic data with auxiliary measurements (e.g., vibration, pressure) to improve identification accuracy
- Robustness enhancement: ensuring adaptability to variable speeds, loads and environmental conditions for broader applicability

Advancements in these areas, particularly through synergies between VMD and machine learning, could revolutionise noise control strategies and thus pave the way for quieter, more efficient and reliable IC engines.

3.4. Machine learning-driven decomposition technologies

Recent years have seen growing interest in applying ML to transform the prediction and diagnostics of engine combustion noise and vibration [96]. In contrast to conventional methods, which are unable to model the intricate, nonlinear relationships between engine operating parameters and noise characteristics, ML techniques, such as artificial neural networks (ANNs), support vector machines (SVMs) and ensemble algorithms, offer data-driven solutions which exhibit superior accuracy and computational efficiency [97].

Uludamar et al. [98] implemented an ANN to evaluate the impact of fuel properties and hydroxy gas addition on the global acceleration of engine vibration. The model exhibited exceptional predictive accuracy, achieving a mean absolute percentage error (MAPE) of only 1.4 % and a correlation coefficient (R^2) of 0.9986 for verification data. This suggests a nearly ideal accord between the predicted and experimental results. M.D. Redel et al. [99] employed product unit neural networks (PUNNs) and radial basis function neural networks (RBFNNs) to predict noise generated by a diesel engine operating on olive pomace oil methyl ester (OPME) and palm oil methyl ester (PME) across different engine configurations. The PUNN model excelled with saturated methyl ester/diesel blends; however, a hybrid model integrating PU and RBF enhanced noise prediction for monounsaturated methyl ester/diesel blends. In the low engine power range, the prediction model for PME (palm oil methyl ester) mixtures exhibited higher relative errors, suggesting limited accuracy. The model is primarily applicable to medium and high engine loading. The hybrid PUNN-RBFNN model is more complex (with more parameters) than the simplified PUNN model, but provides the highest accuracy for monounsaturated methyl ester blends (OPME). The investigation focused on steady-state engine operating conditions, so did not address the transient or dynamic engine conditions prevalent in real-world scenarios. The models may be less sensitive or accurate for certain fuel types and compositions, as the radiated noise by the engine was not significantly influenced by the blend percentage of PME, although the higher content of OPME in the blend increased the noise.

Sefa et al. [100] examined the use of ANNs and SVMs to forecast combined vibration acceleration and overall noise in a diesel engine operating with biodiesel blends and hydrogen enrichment. Engine speed, hydrogen energy substitution rates and biodiesel blend ratios were among the parameters that were varied in the investigation. The comparative analysis demonstrated that the ANN outperformed the SVM, achieving a MAPE of 2.03 % and a R^2 of 0.988 for vibration acceleration, indicating superior predictive accuracy. The ANN model exhibited outstanding performance in predicting overall engine noise, with a relatively low MAPE of 0.28 % and an almost perfect correlation ($R^2 = 0.996$). The robust correlation between experimental data and ANN predictions, as demonstrated by the studýs graphical results, further substantiates the trustworthiness of the ANN methodology for engine noise characterisation. The high costs and time demand of experimentation and data collecting for engine parameters necessitate the use of predictive models, and also constrain availability of extensive datasets for training effective models.

Table 12 summarises the ML-driven decomposition technologies. Machine learning methodologies such as ANN, SVM and hybrid models, can proficiently elucidate intricate, nonlinear correlations between engine parameters and noise/vibration behaviours. Nevertheless, only a limited number of pertinent studies have examined the prediction of combustion-induced noise and vibration, focusing solely on aggregate values. Furthermore, only diesel engines have been investigated in the reviewed studies. Consequently, comprehensive predictions of combustion-induced noise and vibration remain fertile ground for further investigation across diverse

Table 11
Comparison of various VMD technologies for IC engines.

Engine type	Input signal	Analytical approach	Output signal	Application	Validation	Ref.
CI, 6-cyl.	EN	VMD, RobustICA	Noise components of combustion and piston slap	Separation of noise source	CWT, FFT	[16]
CI, 6-cyl.	EN	BSLM, VMD, RobustICA	Noise components of combustion and piston slap	Separation of noise source	CWT, Coherence analysis	[17]
SI, 4-cyl.	VS	WT, VMD	Knock vibration	Identification of knock condition	Knock intensity evaluation	[88]
N/A	EN, VS	VMD, PCA, FAHP	Weighted contributions of various engine components to overall noise	Engine noise source identification and contribution analysis,	Physical phenomena, partial coherent power spectra	[87]
CI, 6-cyl.	EN, VS	Adaptive VMD with FuzzDistEn, PCA,	Identified noise sources	Engine noise source identification	CWT, PCA	[94]
CI, 6-cyl.	VS	VTDD	Engine valve fault signal	Engine valve fault diagnose	FFT	[95]
CI, 6-cyl.	VS	VTFAD	Faults vibration signal	Faults diagnose	Coherence analysis	[31]

Table 12
Comparison of various ML-driven decomposition technologies for IC engines.

Engine type	Input signal	Analytical approach	Output signal	Application	Validation	Ref.
CI, 1-cyl.	Engine speed, flow rate, cetane number of fuels, lower heating value of fuel, VS	ANN, LMA	Predicted VS	Prediction of total acceleration	Data-driven Verification	[98]
CI, 3-cyl.	Speed, engine load, percentage of biodiesel, EN	PUNN, RBFNN, hybrid model, polynomial regression response surface	Predicted EN	Prediction of total acceleration	Verification by test data	[99]
CI, 4-cyl.	Hydrogen energy substitution ratio, engine speed, fuel density, VS, EN	ANN, SVM	Predicted VS, EN	Prediction of overall noise and total acceleration	Comparison with test data	[100]

engine types and operational situations.

4. Discussions

Combustion noise decomposition is essential for improving engine performance, passenger comfort, and reducing environmental noise. Advanced spectrum filters enhance computational efficiency and usability over traditional methods like EMD and VMD by better isolating combustion noise. However, existing combustion noise decomposition techniques still face several major challenges. These include complex operating conditions, algorithmic complexity, limitations in decomposition accuracy, and difficulties in real-time monitoring. Machine learning algorithms offer a promising way to overcome these limitations by improving feature detection and prediction accuracy. This section expands the discussion by evaluating accuracy estimation methods and the role of machine learning in enhancing spectrum filtering for combustion noise decomposition.

Table 13
Analysis of the identification of combustion quantifiers derived from vibration signals.

Combustion quantifier	Identification method	
SOC	Location	zero-crossing point of the filtered acceleration
		the first inflection point in velocity curve
		zero-crossing point in velocity curve
PP	Location	zero-crossing point in vibration velocity curve
		minimum point after peak acceleration
	Value	summation of frequency amplitude
PPRR	Location	peak velocity
		zero-crossing point after peak acceleration
	Value	summation of frequency amplitude
HRRmax	Location	first maximum point in acceleration curve
	Value	cumulative value between 0.3 and 1.5 KHz
		the value of first maximum point in acceleration curve
MFB	Location	MFB50: absolute minimum; MFB95: the following third minimum
	Value	Gaussian probability fit to instantaneous vibration energy, 1.5–3 kHz

4.1. Validation technique for combustion noise decomposition methodology

Section 2 demonstrates a strong correlation between in-cylinder pressure variations and engine block vibrations, as identified through various combustion metrics. Table 13 summarises the methodology for estimating combustion quantifiers from vibration signals. Start of combustion (SOC) can be identified using the zero-crossing point of the filtered acceleration signal or the first inflection point in the velocity curve. Peak pressure (PP) location is identified via the zero-crossing of the velocity curve and the minimum point after peak acceleration; its value is estimated by summing frequency amplitudes. The peak pressure rise rate (PPRR) is estimated from summed frequency amplitudes, with its timing identified by peak velocity and a post-acceleration zero-crossing. The maximum heat release rate (HRRmax) occurs at the first peak in the acceleration curve, and its value is taken at that point. HRRmax also can be estimated using cumulative frequency amplitude between 0.3 and 1.5 kHz. Specific minima in the acceleration signal correspond to MFB50 and MFB95 values. MFB50 can be approximated using a Gaussian fit to vibration energy between 1.5 and 3 kHz.

The estimation accuracy of these quantifiers is superior in CI engines than in engines using other combustion concepts, such as HCCI. Different fuels have distinct properties, resulting in different and challenging combustion phenomena compared with conventional hydrocarbon fuels. Therefore, extensive combustion research is necessary for efficient, stable and robust operation with a specific fuel.

4.2. Integrated perspectives on combustion noise decomposition

It is clear from Section 1́s review that each decomposition approach – filtering, EMD, VMD, and machine learning – has unique strengths but also limitations which hinder its broad applicability.

Filter technologies play a key role in reducing engine noise and improving performance by isolating specific noise sources. However, this strategy requires customised separation filters tailored to different operating conditions. These filters enable precise identification of vibration and noise sources. However, the complexity of the filter model can limit its practical applicability.

Enhanced decomposition methods like EEMD and TVF-EMD address some limitations of classical EMD. They offer better adaptability to complex signals but also increase computational time and complexity. Advancements in these decomposition approaches have expanded the applications of signal processing, which now range from mechanical vibration detection to biological signal analysis. VMD is valuable for improving diagnostics and engine performance due to its robustness to non-stationary, nonlinear, and noisy signals. The separation method is applicable not only for noise analysis but also for feature extraction and defect diagnosis [101,102,103]. This suggests that techniques from other fields could improve precision and efficiency in engine noise separation. Moreover, existing methods for signal decomposition and feature extraction exhibit noticeable deviations and high computational complexity when dealing with impact feature extraction. This primarily is due to the severe frequency aliasing in actual multi-impact signals and the complex nature of impact responses.

Efficiency is a key metric in real-time monitoring of engine performance, since it serves as the foundation for assuring accuracy within the monitoring process. Therefore, the effectiveness of both filter technologies and the VMD method means both approaches can be considered for real-time monitoring of combustion noise. Filtering is the better idea for real-time monitoring to a certain extent, due to the fact that its methodology is both more efficient and simpler. However, high-precision noise extraction requires selection of windows which correspond to the various operating situations, as mentioned earlier. Through the collection of extensive experimental data, machine learning may be utilised to develop a universal filter model that can adapt to a variety of operating parameters, such as engine speed, torque, air–fuel ratio and other factors. This would significantly improve both the feasibility and the spectrum of application of the universal filter model.

Parameter dependence is a characteristic of certain decomposition methods. For instance, the EEMD results are contingent upon the noise amplitude and ensemble number, while the performance of VMD is contingent upon the meticulous adjustment of the balancing parameter (α) and mode number. Genetic algorithms (GA) and reinforcement learning (RL) are among the algorithms that may be implemented to optimise pertinent parameters in this scenario. In addition, research may focus on the further refinement of these methods by training ML models to reduce dimension to optimise the efficacy of computer processes. Additionally, the literature reviewed demonstrates that certain separation methods are solely applicable under specific conditions, such as a particular engine or a defined engine-speed range. This issue can be resolved by employing a variety of research parameters as inputs and utilising machine learning to train existing separation methods. This will expand the applicability of the separation process, enabling its use with advanced combustion concepts, dual-fuel systems and diverse fuel types, among others. The integration of VMD with emerging technologies, such as machine learning, may transform engine noise management strategies, leading to the development of internal combustion engines which are quieter, more efficient and more reliable. This research is currently being undertaken in this domain.

4.2.1. Research gaps and future research directions

Despite progress in vibration-based combustion detection, several key research gaps and future opportunities remain.

1) Decoupling and source identification

A key limitation of variational mode decomposition (VMD) is its strong dependence on predefined parameters, such as the number of modes and penalty factors, which significantly influence decomposition accuracy. Future research therefore should focus on developing adaptive and robust decomposition frameworks which minimise reliance on manual parameter tuning. Integrating optimisation algorithms, – such as genetic algorithms (GA), reinforcement learning (RL) or other metaheuristic approaches, – offers a pathway for automatic parameter selection, enabling decomposition methods to maintain consistent performance across diverse conditions.

In addition, like other signal decomposition techniques, VMD faces challenges when handling highly non-stationary signals where mode mixing and loss of physical interpretability can occur. These issues become more pronounced under varying engine operating conditions due to overlapping frequency bands and interference from mechanical sources such as piston slap and valve dynamics. Therefore, improving source separation and decoupling capabilities is another critical research direction. This would ensure reliable isolation of combustion-related excitations, even in the presence of strong structural and mechanical noise.

2) Reversibility among combustion modes

This work mostly focuses on heavy-duty engine applications, where compression ignition is most commonly used and investigated. However, SI engines are crucial in light-duty vehicles, particularly given advances in pre-chamber ignition, lean burn, and knock control systems. Moreover, the suitability of SI engines for advanced combustion strategies such as dual-fuel systems, RCCI, or HCCI remains underexplored. Validation and benchmarking studies under transient and multi-mode operations are necessary to ensure the robustness of the method. Improving ML model interpretability is crucial to build trust in their predictions.

3) Combustion: real-time virtual sensing

The development of real-time, virtual combustion noise sensors is an intriguing prospect. These could integrate into engine control units by combining pressure and vibration signals for accurate combustion assessments. This integration could facilitate closed-loop combustion noise management and dynamic engine optimisation.

4) Analysing and implementing a machine-learning model

Mapping nonlinear vibration-pressure relationships and automating feature extraction with ML models have shown significant potential. The opaque nature of numerous machine-learning models limits interpretability and undermines real-world confidence in them. Future work should prioritise explainable and hybrid ML models which balance accuracy with transparency and reliability.

5) Multi-sensor fusion and transient operations

Combining vibration signals with other sensory inputs, such as knock sensors, acoustic emissions or optical diagnostics, can improve the dataset and generate more precise combustion characterisation. Model performance and adaptation under transient operating conditions, such as changing engine loads, speeds and environmental factors, should also be studied.

6) Fuel strategy, emission compliance and noise reduction

Predictive models can guide fuel and combustion calibration to reduce engine noise and emissions in order to comply with strict regulations and improvements in environmental performance.

Future research should aim to improve the accuracy, interpretability, and deployment readiness of vibration-based detection systems. This advancement will facilitate the creation of more efficient, quieter, and environmentally friendly internal combustion engines.

5. Conclusions

This review focused on the urgent need for non-intrusive combustion event detection in compression ignition (CI) and homogeneous charge compression ignition (HCCI) engines. The study links vibration signals with combustion characteristics, aiming to support the development of affordable, scalable alternatives to traditional in-cylinder pressure sensors. Each research objective was supported through a comprehensive literature review.

Related to objective 1: The review established quantitative validation of the relationship between engine-block vibrations and combustion parameters, including SOC; PP; PPRR; HRRmax; and MFB. Results confirmed vibration signals as reliable combustion indicators. For example, SOC and LOPP errors were under 0.9 CAD, PP within 4.93 % and HRRmax location errors were within 0.62 CAD.

Related to objective 2: The aim was to benchmark several signal decomposition techniques to assess their capacity to separate mechanical noise from combustion-induced vibrations. VMD and EMD consistently outperformed other methods, with combustion feature extraction errors under 1 CAD. Still, operational conditions, transfer path properties and the complexity of combustion dynamics, especially in HCCI modes, all affect decomposition accuracy.

Related to objective 3: The vibration-based quantifiers most appropriate for real-time monitoring were found and ranked, based on estimation accuracy, signal-to-noise ratio and cost of implementation. Zero-crossing analysis of filtered acceleration provides sub-0.9 CAD accuracy for SOC and PP, making it well-suited for onboard diagnostics.

Related to objective 4: The study evaluated the impacts on vibration-based sensing systems of transient operating circumstances and advanced combustion modes (e.g., LTC, HCCI, RCCI). While CI engines showed stable estimates, HCCI engines had more variation (SOC errors: 2.4–3.3 CAD), highlighting the need for combustion-mode-specific data processing.

Related to objective 5: Machine-learning models, particularly RBF and GRNN networks, significantly improved reconstruction accuracy. Studies obtained RMSEs for peak pressure below 3.9 % and MFB50 timing within 1.6 CAD, therefore illustrating the potential of hybrid approaches combining ML with decomposition techniques for strong, nonlinear mapping.

This review shows that with advanced signal processing and modelling, vibration-based combustion analysis is nearly ready for widespread implementation. As part of the shift to cleaner, more efficient combustion strategies, this technology offers a viable path for next-generation ICE diagnostics, achieving sub-1 CAD estimation errors and under 5 % RMSE for pressure reconstruction.

CRediT authorship contribution statement

Zengquan Zheng: Writing – original draft, Visualization, Validation, Methodology, Investigation, Formal analysis, Data curation, Conceptualization. **Petros Lappas:** Writing – review & editing, Validation, Software. **Amir-Mohammad Shamekhi:** Writing – review

& editing, Supervision, Project administration, Methodology, Formal analysis, Conceptualization. **Xu Wang:** Writing – review & editing, Validation, Supervision, Resources, Project administration, Methodology, Formal analysis, Conceptualization. **Maciej Mikulski:** Writing – review & editing, Supervision, Resources, Project administration, Funding acquisition, Conceptualization.

Declaration of competing interest

The authors declare that they have no known competing financial interests or personal relationships that could have appeared to influence the work reported in this paper.

Acknowledgements

This paper is supported by Business Finland, Silent Engine Project. This paper has received funding from the European Union's Horizon 2020 research and innovation programme, within the OpenInnoTrain project under the Marie Skłodowska-Curie grant agreement No. 823971. The authors would also like to thank David for his valuable assistance in improving the language and clarity of this paper. The content of this publication does not reflect the official opinion of the European Union.

Data availability

No data was used for the research described in the article.

References

[1] C. Fang, M. Ouyang, F. Yang, Real-time start of combustion detection based on cylinder pressure signals for compression ignition engines, Appl. Therm. Eng. 114 (2017) 264–270.
[2] H.N. Gupta, *Fundamentals of internal combustion engines*, Second. PHI Learning Pvt. Ltd. (2012).
[3] C. Guardiola, B. Pla, P. Bares, A. Barbier, Closed-loop control of a dual-fuel engine working with different combustion modes using in-cylinder pressure feedback, Int. J. Engine Res. 21 (3) (Mar. 2019) 484–496, https://doi.org/10.1177/1468087419835327.
[4] R.K. Maurya, A.K. Agarwal, Investigations on the effect of measurement errors on estimated combustion and performance parameters in HCCI combustion engine, Measurement 46 (1) (2013) 80–88, https://doi.org/10.1016/j.measurement.2012.05.021.
[5] S. Kulah, A. Forrai, F. Rentmeester, T. Donkers, F. Willems, Robust cylinder pressure estimation in heavy-duty diesel engines, Int. J. Engine Res. 19 (2) (2018) 179–188, https://doi.org/10.1177/1468087417713336.
[6] X.T. Dong, M.H. Nguyen, D. Lee, Algorithm development for acoustic emission measurement in high-frequency ranges and its application on a large two-stroke marine diesel engine, Measurement 162 (2020) 107907, https://doi.org/10.1016/j.measurement.2020.107907.
[7] N. Sharma, C. Patel, N. Tiwari, A.K. Agarwal, Experimental investigations of noise and vibration characteristics of gasoline-methanol blend fuelled gasoline direct injection engine and their relationship with combustion characteristics, Appl. Therm. Eng. 158 (2019) 113754, https://doi.org/10.1016/j.applthermaleng.2019.113754.
[8] S. Delvecchio, P. Bonfiglio, F. Pompoli, Vibro-acoustic condition monitoring of internal combustion engines: a critical review of existing techniques, Mech. Syst. Signal Process. 99 (2018) 661–683, https://doi.org/10.1016/j.ymssp.2017.06.033.
[9] M. Jia, M. Xie, H. Liu, W.H. Lam, T. Wang, Numerical simulation of cavitation in the conical-spray nozzle for diesel premixed charge compression ignition engines, Fuel 90 (8) (Aug. 2011) 2652–2661, https://doi.org/10.1016/j.fuel.2011.04.017.
[10] A.K.S. Jardine, D. Lin, D. Banjevic, A review on machinery diagnostics and prognostics implementing condition-based maintenance, Mech. Syst. Signal Process. 20 (7) (2006) 1483–1510, https://doi.org/10.1016/j.ymssp.2005.09.012.
[11] Z. Wang, H. Liu, R.D. Reitz, Knocking combustion in spark-ignition engines, Prog. Energy Combust. Sci. 61 (2017) 78–112, https://doi.org/10.1016/j.pecs.2017.03.004.
[12] B.C. Kaul, B. Lawler, A. Zahdeh, Engine diagnostics using acoustic emissions sensors, SAE Int. J. Engines 9 (2) (2016) 684–692, https://doi.org/10.4271/2016-01-0639.
[13] N. Cavina, A. Businaro, N. Rojo, M. De Cesare, L. Paiano, A. Cerofolini, Combustion and intake/exhaust systems diagnosis based on acoustic emissions of a GDI TC engine, Energy Procedia 101 (2016) 677–684.
[14] F. Bi, L. Li, J. Zhang, T. Ma, Source identification of gasoline engine noise based on continuous wavelet transform and EEMD-RobustICA, Appl. Acoust. 100 (Dec. 2015) 34–42, https://doi.org/10.1016/j.apacoust.2015.07.007.
[15] E. Di Giulio, R. Di Leva, R. Dragonetti, Theoretical and experimental assessment of nonlinear acoustic effects through an orifice, Acoustics 6 (4) (2024) 818–833, https://doi.org/10.3390/acoustics6040046.
[16] J. Yao, Y. Xiang, S. Qian, S. Wang, S. Wu, Noise source identification of diesel engine based on variational mode decomposition and robust independent component analysis, Appl. Acoust. 116 (Jan. 2017) 184–194, https://doi.org/10.1016/j.apacoust.2016.09.026.
[17] J. Yao, Y. Xiang, S. Qian, S. Li, S. Wu, Noise source separation of diesel engine by combining binaural sound localization method and blind source separation method, Mech. Syst. Signal Process. 96 (Nov. 2017) 303–320, https://doi.org/10.1016/j.ymssp.2017.04.027.
[18] Z.L. Tang, et al., Identifying fault cylinder location of diesel engines based on instantaneous speed, Mech. Syst. Signal Process. 225 (Feb. 2025), https://doi.org/10.1016/j.ymssp.2025.112301.
[19] Y. Li, Z. Guo, Z. Li, Z. Deng, K. Noman, Instantaneous angular speed-based fault diagnosis of multicylinder marine diesel engine using intrinsic multiscale dispersion entropy, IEEE Sens. J. 23 (9) (2023) 9523–9535.
[20] H. Zhao, N. Ladommatos, Optical diagnostics for in-cylinder mixture formation measurements in IC engines, Prog. Energy Combust. Sci. 24 (4) (1998) 297–336.
[21] K. Kumano, Y. Akagi, S. Matohara, Y. Uchise, Y. Yamasaki, Using an ion-current sensor integrated in the ignition system to detect precursory phenomenon of pre-ignition in gasoline engines, Appl. Energy 275 (2020) 115341.
[22] R. Han, C. Bohn, G. Bauer, "Recursive Engine In-Cylinder pressure Estimation using Kalman Filter and Structural Vibration Signal," in *IFAC-Papers OnLine*, Elsevier b.v., Jan. (2018) 700–705, https://doi.org/10.1016/j.ifacol.2018.10.161.
[23] C. Bennett, J.F. Dunne, S. Trimby, D. Richardson, Engine cylinder pressure reconstruction using crank kinematics and recurrently-trained neural networks, Mech. Syst. Signal Process. 85 (2017) 126–145, https://doi.org/10.1016/j.ymssp.2016.07.015.
[24] K. Bizon, G. Continillo, E. Mancaruso, B.M. Vaglieco, "Reconstruction of in-cylinder pressure in a diesel engine from vibration signal using a RBF neural network model," in *SAE Technical Papers*, SAE International (2011), https://doi.org/10.4271/2011-24-0161.
[25] H.K. Nguyen, A. Modabberian, K. Zenger, É. Lendormy, M. Mikulski, J. Hunicz, "A Neural Network Approach for Reconstructing In-Cylinder pressure from Engine Vibration Data," in *SAE Technical Papers*, SAE International (Aug. 2022), https://doi.org/10.4271/2022-01-1038.

[26] H. Bendu, B.B.V.L. Deepak, S. Murugan, Application of GRNN for the prediction of performance and exhaust emissions in HCCI engine using ethanol, Energy Convers. Manage. 122 (2016) 165–173, https://doi.org/10.1016/j.enconman.2016.05.061.

[27] F. Bi, T. Ma, X. Wang, Development of a novel knock characteristic detection method for gasoline engines based on wavelet-denoising and EMD decomposition, Mech. Syst. Signal Process. 117 (Feb. 2019) 517–536, https://doi.org/10.1016/j.ymssp.2018.08.008.

[28] K. Dragomiretskiy, D. Zosso, Variational mode decomposition, IEEE Trans. Signal Process. 62 (3) (Feb. 2014) 531–544, https://doi.org/10.1109/TSP.2013.2288675.

[29] J. Hunicz, M.S. Gęca, E. Ratajczyk, A.M. Andwari, L. Yang, M. Mikulski, An analytical approach to converting vibration signal to combustion characteristics of homogeneous charge compression ignition engines, Energy Convers. Manage. 294 (Oct. 2023) 117564, https://doi.org/10.1016/j.enconman.2023.117564.

[30] Z. Wu, N.E. Huang, Ensemble empirical mode decomposition: a noise assisted data analysis method, Adv. Adapt. Data Anal. 1 (1) (2009) 1–41, https://doi.org/10.1142/S1793536909000047.

[31] N. Zhao, J. Zhang, Z. Mao, Z. Jiang, Variational time–frequency adaptive decomposition of machine multi-impact vibration signals, Mech. Syst. Signal Process. 189 (Apr. 2023), https://doi.org/10.1016/j.ymssp.2022.110084.

[32] Y. Sheng Yang, A. Bo Ming, Y. Yun Zhang, Y. Sheng Zhu, "Discriminative non-negative matrix factorization (DNMF) and its application to the fault diagnosis of diesel engine," Mech Syst Signal Process, vol. 95, pp. 158–171, Oct. 2017, doi: 10.1016/j.ymssp.2017.03.026.

[33] G. Shibata, H. Ogawa, Y. Amanuma, Y. Okamoto, Optimization of multiple heat releases in pre-mixed diesel engine combustion for high thermal efficiency and low combustion noise by a genetic-based algorithm method, Int. J. Engine Res. 20 (5) (2019) 540–554, https://doi.org/10.1177/1468087418767225.

[34] U. Asad, P. Divekar, M. Zheng, J. Tjong, Low temperature combustion strategies for compression ignition engines: operability limits and challenges, SAE Technical Paper (2013).

[35] M. Punasiya, A.K. Sarangi, Machine learning-based modeling and predictive control of combustion phasing and load in a dual-fuel low-temperature combustion engine, SAE Int. J. Engines, vol. 17, no. 03-17-04–0030, 2024.

[36] P.A. Lakshminarayanan, Study of noise and vibration problems related to heavy duty diesel engines, in Design and Development of Heavy Duty Diesel Engines: A Handbook, Springer, 2019, pp. 833–884.

[37] T. Chu, T. Nguyen, H. Yoo, J. Wang, A review of vibration analysis and its applications, Heliyon, 10(5), 2024.

[38] Y.E. Karabacak, Condition monitoring of internal combustion engines with vibration signals and fault detection by using machine learning techniques, Int. J. Automotive Eng. Technol. 13 (4) (2024) 191–200, https://doi.org/10.18245/ijaet.1251886.

[39] G. Chiatti, O. Chiavola, E. Recco, A. Magno, E. Mancaruso, B.M. Vaglieco, Accelerometer measurement for MFB evaluation in multi-cylinder diesel engine, Energy 133 (2017) 843–850, https://doi.org/10.1016/j.energy.2017.04.148.

[40] S. Ji, et al., Study on the relationship between combustion parameters and cylinder head vibration signal in time domain, Energies (Basel) 14 (19) (2021), https://doi.org/10.3390/en14196421.

[41] J.M. Lujan, V. Bermúdez, C. Guardiola, A. Abbad, A methodology for combustion detection in diesel engines through in-cylinder pressure derivative signal, Mech. Syst. Signal Process. 24 (7) (2010) 2261–2275, https://doi.org/10.1016/j.ymssp.2009.12.012.

[42] X. Zhao, Y. Cheng, L. Wang, S. Ji, Real time identification of the internal combustion engine combustion parameters based on the vibration velocity signal, J. Sound Vib. 390 (Mar. 2017) 205–217, https://doi.org/10.1016/j.jsv.2016.11.013.

[43] W. Yang, C. Yong, Vibration analysis and combustion parameter evaluation of CI engine based on Fourier decomposition method, Int. J. Engine Res. 23 (3) (Mar. 2022) 434–445, https://doi.org/10.1177/1468087420988195.

[44] Y. Cheng, J. Tang, S. Ji, M. Huang, Combustion timing determination based on vibration velocity in HCCI engines, Mech. Mach. Theory 58 (Dec. 2012) 20–28, https://doi.org/10.1016/j.mechmachtheory.2012.08.004.

[45] S. Ji, et al., Combustion parameter estimation for ICE from surface vibration using frequency spectrum analysis, Measurement (Lond) 128 (Nov. 2018) 485–494, https://doi.org/10.1016/j.measurement.2018.07.002.

[46] S. Lee, Y. Lee, S. Lee, H.H. Song, K. Min, H. Choi, "Study on the Correlation between the Heat Release Rate and Vibrations from a Diesel Engine Block," in *SAE Technical Papers*, SAE International (Apr. 2015), https://doi.org/10.4271/2015-01-1673.

[47] K.Z. Mendera, A. Spyra, M. Smereka, Mass fraction burned analysis, J. KONES Internal Combustion Engines, vol. 3, no. 4, pp. 193–201, 2002, [Online]. Available: https://citeseerx.ist.psu.edu/document?repid=rep1&type=pdf&doi=096f671df503ee7dc8161665226022eeca8489a1.

[48] J. Chauvin, O. Grondin, E. Nguyen, F. Guillemin, Real-time combustion parameters estimation for HCCI-diesel engine based on knock sensor measurement, in: In *IFAC Proceedings Volumes (IFAC-Papers Online)*, 2008, https://doi.org/10.3182/20080706-5-KR-1001.1789.

[49] R.J. Liu, Z.Y. Hao, X. Zheng, H. Su, H.F. Jiang, Investigation of idling vibration characteristics of gasoline engine based on adaptive generalized S transform, Zhejiang Daxue Xuebao (Gongxue Ban)/Journal of Zhejiang University (Engineering Science), vol. 50, no. 3, pp. 460–467, Mar. 2016, doi: 10.3785/j.issn.1008-973X.2016.03.009.

[50] X. Zheng, N. Zhou, Q. Zhou, Y. Qiu, R. Liu, Z. Hao, Experimental investigation on the high-frequency pressure oscillation characteristics of a combustion process in a di diesel engine, Energies (Basel), 13(4), 2020, doi: 10.3390/en13040871.

[51] J. Antoni, J. Daniere, F. Guillet, Effective vibration analysis of IC engines using cyclostationarity. Part I-A methodology for condition monitoring, J. Sound Vib. 5 (2002) 815–837, https://doi.org/10.1006/jsvi.5062.

[52] J. Antoni, J. Daniere, F. Guillet, R.B. Randall, Effective vibration analysis of IC engines using cyclostationarity. Part II-new results on the reconstruction of the cylinder pressures, J. Sound Vib. 5 (2002) 839–856, https://doi.org/10.1006/jsvi.5063.

[53] Q. Zhang, Z. Hao, X. Zheng, W. Yang, Characteristics and effect factors of pressure oscillation in multi-injection DI diesel engine at high-load conditions, Appl. Energy 195 (2017) 52–66, https://doi.org/10.1016/j.apenergy.2017.03.048.

[54] R.G. DeJong, R.E. Powell, J.E. Manning, Engine monitoring using vibration signals, SAE Transactions, pp. 1059–1065, 1986, [Online]. Available: http://www.jstor.org/stable/44469117.

[55] R.H. Lyon, J.T. Kim, Recovery of fault signatures in diesel engines, SAE Technical Paper (1988), https://doi.org/10.4271/880824.

[56] P. Azzoni, G. Cantoni, G. Minelli, E. Padovani, Cylinder pressure signal recovering from vibration signals, in Proceedings of the 20th International Symposium on Automotive technology and automation, Florence, 1989.

[57] D. L. Bowen and MFPG., Recovery of Combustion Pressure from Diesel Engine Vibration, in Proceedings of 45th Meeting of the Mechanical Failures Prevention Group, Mechanical Failures Prevention Group, 1991.

[58] C.R.E.E. Clementel, Reconstruction of indicated pressure waveform in a spark-ignition engine from block vibration measurements, J. Dyn. Syst. Meas. Control. 119 (4) (1997) 614–619, https://doi.org/10.1115/1.2802369.

[59] Y. Gao, R.B. Randall, Reconstruction of diesel engine cylinder pressure using a time domain smoothing technique, Mech. Syst. Signal Process. 13 (5) (1999) 709–722, https://doi.org/10.1006/mssp.1999.1229.

[60] G.Z. Villarroel, A. Ågren, B.B. Randall, Y. Gao, Reconstruction of cylinder pressure time trace on a six-cylinder engine from acceleration measurements, in Proceedings of the International Conference on Noise and Vibration Engineering (ISMA), Leuven, Belgium: Katholieke Universiteit Leuven, 1998, pp. 331–337.

[61] M. El-Ghamry, J.A. Steel, R.L. Reuben, T.L. Fog, Indirect measurement of cylinder pressure from diesel engines using acoustic emission, Mech. Syst. Signal Process. 19 (4) (Jul. 2005) 751–765, https://doi.org/10.1016/j.ymssp.2004.09.004.

[62] A.B. Badawi, A. Elmaihy, A.S. Samy, M.A. Shahin, K.I. Mohamed, Reconstruction of diesel engine cylinder pressure using vibration and acoustic emission, in: In *12th International Conference on Applied Mechanics and Mechanical Engineering (AMME)*, 2006, pp. 510–525, https://doi.org/10.21608/amme.2006.41368.

[63] G. Zurita, D. Haupt, and A. Ågren, "Reconstruction of cylinder pressure through multivariate data analysis: For prediction of noise and exhaust emissions," 2004. [Online]. Available: https://www.researchgate.net/profile/Grover-Zurita/publication/269519032_Reconstruction_of_the_Cylinder_Pressure_from_Vibration_Measurements_for_Prediction_of_Exhaust_and_Noise_Emissions_in_Ethanol_Engines/links/565cb62408aefe619b253be0/Reconstruction-of-the-Cylinder-Pressure-from-Vibration-Measurements-for-Prediction-of-Exhaust-and-Noise-Emissions-in-Ethanol-Engines.pdf.

[64] H. Du, L. Zhang, and X. Shi, "Reconstructing cylinder pressure from vibration signals based on radial basis function networks," *Proceedings of the Institution of Mechanical Engineers, Part D: Journal of automobile engineering*, vol. 215, no. 6, pp. 761–767, 2001, doi: 10.1243/0954407011528338.

[65] J. C. Peña and G. Zurita, "Vibration based reconstruction of the cylinder pressure in diesel engines by using neural networks," *Revista Investigación & Desarrollo*, vol. 1, no. 5, pp. 81–89, 2005, [Online]. Available: https://www1.upb.edu/revista-investigacion-desarrollo/index.php/id/article/view/116.
[66] R. Johnsson, Cylinder pressure reconstruction based on complex radial basis function networks from vibration and speed signals, Mech. Syst. Signal Process. 20 (8) (Nov. 2006) 1923–1940, https://doi.org/10.1016/j.ymssp.2005.09.003.
[67] K. Bizon, G. Continillo, E. Mancaruso, B.M. Vaglieco, "Towards on-line prediction of the in-cylinder pressure in diesel engines from engine vibration using artificial neural networks," in *SAE Technical Papers*, SAE International (2013), https://doi.org/10.4271/2013-24-0137.
[68] S. Trimby, J.F. Dunne, C. Bennett, D. Richardson, Unified approach to engine cylinder pressure reconstruction using time-delay neural networks with crank kinematics or block vibration measurements, Int. J. Engine Res. 18 (3) (Mar. 2017) 256–272, https://doi.org/10.1177/1468087416655013.
[69] E. Song, X.Y. Liu, L. Tang, C. Yao, P. Xu, Cylinder pressure reconstruction to compensate for crankshaft flexibility based on flexible crank model, Int. J. Engine Res. (Oct. 2024), https://doi.org/10.1177/14680874241257315.
[70] F. Ricci, M. Avana, and F. Mariani, "Artificial neural networks as a tool for high-accuracy prediction of in-cylinder pressure and equivalent flame radius in hydrogen-fueled internal combustion engines," *Energies (Basel)*, vol. 18, no. 2, Jan. 2025, doi: 10.3390/en18020299.
[71] H. Vafamehr, A. Cairns, O. Sampson, M.M. Koupaie, The competing chemical and physical effects of transient fuel enrichment on heavy knock in an optical spark ignition engine, Appl. Energy 179 (2016) 687–697.
[72] F. Bozza, V. De Bellis, L. Teodosio, Potentials of cooled EGR and water injection for knock resistance and fuel consumption improvements of gasoline engines, Appl. Energy 169 (2016) 112–125.
[73] S. Beccari, E. Pipitone, G. Genchi, Knock onset prediction of propane, gasoline and their mixtures in spark ignition engines, J. Energy Inst. 89 (1) (2016) 101–114.
[74] I. Tougri, M.J. Colaço, A.J.K. Leiroz, T.C.C. Melo, Knocking prediction in internal combustion engines via thermodynamic modeling: preliminary results and comparison with experimental data, J. Braz. Soc. Mech. Sci. Eng. 39 (1) (2017) 321–327, https://doi.org/10.1007/s40430-016-0519-5.
[75] J.M. Luján, C. Guardiola, B. Pla, P. Bares, Estimation of trapped mass by in-cylinder pressure resonance in HCCI engines, Mech. Syst. Signal Process. 66 (2016) 862–874.
[76] P. Kyrtatos, C. Brückner, K. Boulouchos, Cycle-to-cycle variations in diesel engines, Appl. Energy 171 (2016) 120–132, https://doi.org/10.1016/j.apenergy.2016.03.015.
[77] I. Jung, J. Jin, K. Won, S. Yang, K. Min, H. Choi, "Closed-loop control for diesel combustion noise using engine vibration signals," in *SAE Technical Papers*, SAE International (Jun. 2015), https://doi.org/10.4271/2015-01-2297.
[78] L. Pruvost, Q. Leclère, E. Parizet, Diesel engine combustion and mechanical noise separation using an improved spectrofilter, Mech. Syst. Signal Process. 23 (7) (Oct. 2009) 2072–2087, https://doi.org/10.1016/j.ymssp.2009.04.001.
[79] J. Antoni, N. Ducleaux, G. Nghiem, S. Wang, Separation of combustion noise in IC engines under cyclo-non-stationary regime, Mech. Syst. Signal Process. 38 (1) (Jul. 2013) 223–236, https://doi.org/10.1016/j.ymssp.2013.02.015.
[80] X. Liu, R.B. Randall, Blind source separation of internal combustion engine piston slap from other measured vibration signals, Mech. Syst. Signal Process. 19 (6) (Nov. 2005) 1196–1208, https://doi.org/10.1016/j.ymssp.2005.08.004.
[81] X. Zhang, Z. Liu, Q. Miao, L. Wang, An optimized time varying filtering based empirical mode decomposition method with grey wolf optimizer for machinery fault diagnosis, J. Sound Vib. 418 (2018) 55–78, https://doi.org/10.1016/j.jsv.2017.12.028.
[82] H. Li, Z. Li, W. Mo, A time varying filter approach for empirical mode decomposition, Signal Process. 138 (2017) 146–158.
[83] Y. Xu, Z. Cai, K. Ding, An enhanced bearing fault diagnosis method based on TVF-EMD and a high-order energy operator, Meas. Sci. Technol. 29 (9) (2018) 095108, https://doi.org/10.1088/1361-6501/aad499.
[84] W. Zheng, et al., Composite quantile regression extreme learning machine with feature selection for short-term wind speed forecasting: a new approach, Energy Convers Manag 151 (2017) 737–752, https://doi.org/10.1016/j.enconman.2017.09.029.
[85] M. Lazhari, A. Sadhu, Decentralized modal identification of structures using an adaptive empirical mode decomposition method, J. Sound Vib. 447 (May 2019) 20–41, https://doi.org/10.1016/j.jsv.2019.01.049.
[86] J. Yao, Y. Xiang, S. Qian, S. Wang, Noise source separation of an internal combustion engine based on a single-channel algorithm, Shock Vib. 2019 (2019), https://doi.org/10.1155/2019/1283263.
[87] J. Zhang, Q. Zhou, J. Lin, W. Li, Z. Tang, C. Duan, A fuzzy-based analytic hierarchy process for mechanical noise source identification of a diesel engine, Shock Vib. 2019 (2019), https://doi.org/10.1155/2019/2854836.
[88] J. Sun, X. Zhang, Q. Tang, Y. Wang, Y. Li, Knock recognition of knock sensor signal based on wavelet transform and variational mode decomposition algorithm, Energy Convers Manag 287 (Jul. 2023), https://doi.org/10.1016/j.enconman.2023.117062.
[89] J. Lian, Z. Liu, H. Wang, X. Dong, Adaptive variational mode decomposition method for signal processing based on mode characteristic, Mech. Syst. Signal Process. 107 (Jul. 2018) 53–77, https://doi.org/10.1016/j.ymssp.2018.01.019.
[90] P. Shi, W. Yang, Precise feature extraction from wind turbine condition monitoring signals by using optimised variational mode decomposition, IET Renew. Power Gener. 11 (3) (Feb. 2017) 245–252, https://doi.org/10.1049/iet-rpg.2016.0716.
[91] C. Yi, Y. Lv, Z. Dang, A fault diagnosis scheme for rolling bearing based on particle swarm optimization in variational mode decomposition, Shock Vib. 2016 (2016), https://doi.org/10.1155/2016/9372691.
[92] X. Zheng, Q. Zhou, N. Zhou, R. Liu, Z. Hao, and Y. Qiu, "A dichotomy-based variational mode decomposition method for rotating machinery fault diagnosis, Meas. Sci. Technol., 31(1), 2020, doi: 10.1088/1361-6501/ab3d04.
[93] X. Zheng, Q. Zhou, Z. Hao, Y. Qiu, Research on mechanism diagnosis of an idling abnormal noise of automobile engine, Appl. Acoust. 171 (Jan. 2021), https://doi.org/10.1016/j.apacoust.2020.107670.
[94] Q. Zhou, J. Zhang, T. Zhou, Y. Qiu, H. Jia, J. Lin, A parameter-adaptive variational mode decomposition approach based on weighted fuzzy-distribution entropy for noise source separation, Meas. Sci. Technol. 31 (12) (2020) Dec, https://doi.org/10.1088/1361-6501/aba3f3.
[95] N. Zhao, J. Zhang, W. Ma, Z. Jiang, Z. Mao, Variational time-domain decomposition of reciprocating machine multi-impact vibration signals, Mech. Syst. Signal Process. 172 (Jun. 2022), https://doi.org/10.1016/j.ymssp.2022.108977.
[96] H. Mohasab, M. Abouelsoud, A.N. Shmroukh, N.M. Ghazaly, Application of artificial neural networks in predicting internal combustion engine performance and emission characteristics: a review of key methodologies and findings, Int. J. Robotics Control Syst. 4 (4) (2024) 1967–2025, https://doi.org/10.31763/ijrcs.v4i4.1584.
[97] A.N. Bhatt, N. Shrivastava, Application of artificial neural network for internal combustion engines: a state of the art review, Arch. Comput. Meth. Eng. 29 (2) (Mar. 2022) 897–919, https://doi.org/10.1007/s11831-021-09596-5.
[98] E. Uludamar, et al., Evaluation of vibration characteristics of a hydroxyl (HHO) gas generator installed diesel engine fuelled with different diesel–biodiesel blends, Int. J. Hydrogen Energy 42 (36) (Sep. 2017) 23352–23360, https://doi.org/10.1016/j.ijhydene.2017.01.192.
[99] M.D. Redel-Macías, C. Hervás-Martínez, P.A. Gutiérrez, S. Pinzi, A.J. Cubero-Atienza, M.P. Dorado, Computational models to predict noise emissions of a diesel engine fueled with saturated and monounsaturated fatty acid methyl esters, Energy 144 (Feb. 2018) 110–119, https://doi.org/10.1016/j.energy.2017.11.143.
[100] S. Yıldırım, E. Tosun, A. Çalık, İ. Uluocak, E. Avşar, Artificial intelligence techniques for the vibration, noise, and emission characteristics of a hydrogen-enriched diesel engine, Energy Sources Part A 41 (18) (Sep. 2019) 2194–2206, https://doi.org/10.1080/15567036.2018.1550540.
[101] G. Li, G. Tang, G. Luo, H. Wang, Underdetermined blind separation of bearing faults in hyperplane space with variational mode decomposition, Mech. Syst. Signal Process. 120 (2019) 83–97, https://doi.org/10.1016/j.ymssp.2018.10.016.
[102] S. Wang, B. Zhao, Y. Luo, Wind turbine gearbox fault diagnosis based on the vibration spectrum analysis, J. Comput. Methods Sci. Eng. 19 (2019) 137–151, https://doi.org/10.3233/JCM-180856.
[103] T. Liu, Y.C. Jin, S. Wang, Q.W. Zheng, G. Yang, Denoising method of weak fault acoustic emission signal under strong background noise of engine based on autoencoder and wavelet packet decomposition, Struct. Health Monit. 22 (5) (Sep. 2023) 3206–3224, https://doi.org/10.1177/14759217221143547.